A near real-time drought monitoring system for Spain using automatic weather station network

S. M. Vicente-Serrano, F. Domínguez-Castro, F. Reig, S. Beguería, M. Tomas-Burguera, B. Latorre, D. Peña-Angulo, I. Noguera, I. Rabanaque, Y. Luna, et al.

Atmospheric Research 271 (2022) 106095

Contents lists available at ScienceDirect

Atmospheric Research

journal homepage: www.elsevier.com/locate/atmosres

A near real-time drought monitoring system for Spain using automatic weather station network

S.M. Vicente-Serrano [a,*], F. Domínguez-Castro [b,c], F. Reig [a], S. Beguería [d], M. Tomas-Burguera [e], B. Latorre [d], D. Peña-Angulo [f], I. Noguera [a], I. Rabanaque [c], Y. Luna [g], A. Morata [g], A. El Kenawy [h]

[a] Instituto Pirenaico de Ecología, Consejo Superior de Investigaciones Científicas (IPE–CSIC), Zaragoza, Spain
[b] Aragonese Agency for Research and Development Researcher (ARAID), Spain
[c] Department of Geography, University of Zaragoza, Zaragoza, Spain
[d] Estación Experimental de Aula Dei, Consejo Superior de Investigaciones Científicas (EEAD–CSIC), Zaragoza, Spain
[e] CNRM - Université de Toulouse, Météo-France/CNRS, Toulouse, Occitanie, France
[f] HSM, Université de Montpellier, CNRS, IRD, Montpellier, France
[g] Agencia Estatal de Meteorología, Leonardo Prieto Castro, 8, 28040 Madrid, Spain
[h] Department of Geography, Mansoura University, Mansoura, Egypt

ARTICLE INFO

Keywords:
Drought monitoring
Meteorological drought
Surface observations
SPI
SPEI
Spain

ABSTRACT

Drought monitoring is essential to determine, at short time intervals, the main characteristics of drought events, such as their duration, severity, and spatial distribution. To ensure that drought monitoring represents a useful tool for governmental plans aimed at preventing or minimizing drought impacts, up-to-date information must be instantaneously accessible and it must provide high spatial and temporal resolution. This study presents a system that allows the automatic tracking of meteorological droughts in the Spanish territory, based on an open and easy-to-use online platform (https://monitordesequia.csic.es/monitor). This drought monitoring system provides two drought synthetic indices: the Standardised Precipitation Index (SPI) and the Standardised Precipitation Evapotranspiration Index (SPEI). Information is provided on a quasi-weekly basis, in a grid format, with a spatial resolution of 1.1*1.1 km, and with data from 1961 to the present time. This drought monitor is updated based on the real-time information gathered from automatic stations, which in turn requires historic information to identify and track drought events. The drought indices are obtained from data processing (quality control, temporal series reconstruction, homogenisation, interpolation, and validation) using climatic variables (maximum and minimum temperatures, solar radiation, rainfall, dew point, and wind speed) which are provided by the Spanish Meteorology Agency and the Ministry of Agriculture of the Spanish Government. We performed a validation of the drought indices for the whole historical period (1961–2020). This allowed us to observe a strong spatial agreement between the indices obtained with the historical dataset and the indices from the monitoring dataset, especially for mainland Spain and the Balearic Islands (Pearson's r, SPI and SPEI >0.99). The presented real-time drought monitoring system represents a relevant and useful tool that allows for quick and effective actions to prevent and mitigate the effects of drought on society and ecosystems.

1. Introduction

Drought monitoring (DM) refers to the real-time quantification of drought severity over a territory (Wood et al., 2015). A drought monitoring system (DMS) must thus allow the determination of drought onset and characterisation of its spatial extent and severity at any given moment. DMSs are a prerequisite for implementing drought plans since any institutional decisions (e.g., alarm declaration, water restrictions, subsidies, etcetera) need to be based on accurate and objective information (Wilhite, 2009). Therefore, DMSs are also fundamental tools to improve drought adaptation and develop mitigation measures (Bokal et al., 2014; Dracup, 1991). Other desirable characteristics of drought monitoring systems are having an open and user-friendly platform (Bachmair et al., 2016a, 2016b) or data retrieval and analysis capacities to help decision support tools (Hervás-Gámez and Delgado-Ramos, 2019; Pulwarty and Sivakumar, 2014; Wilhite, 2007).

* Corresponding author.
E-mail address: svicen@ipe.csic.es (S.M. Vicente-Serrano).

https://doi.org/10.1016/j.atmosres.2022.106095
Received 15 November 2021; Received in revised form 27 January 2022; Accepted 20 February 2022
Available online 22 February 2022

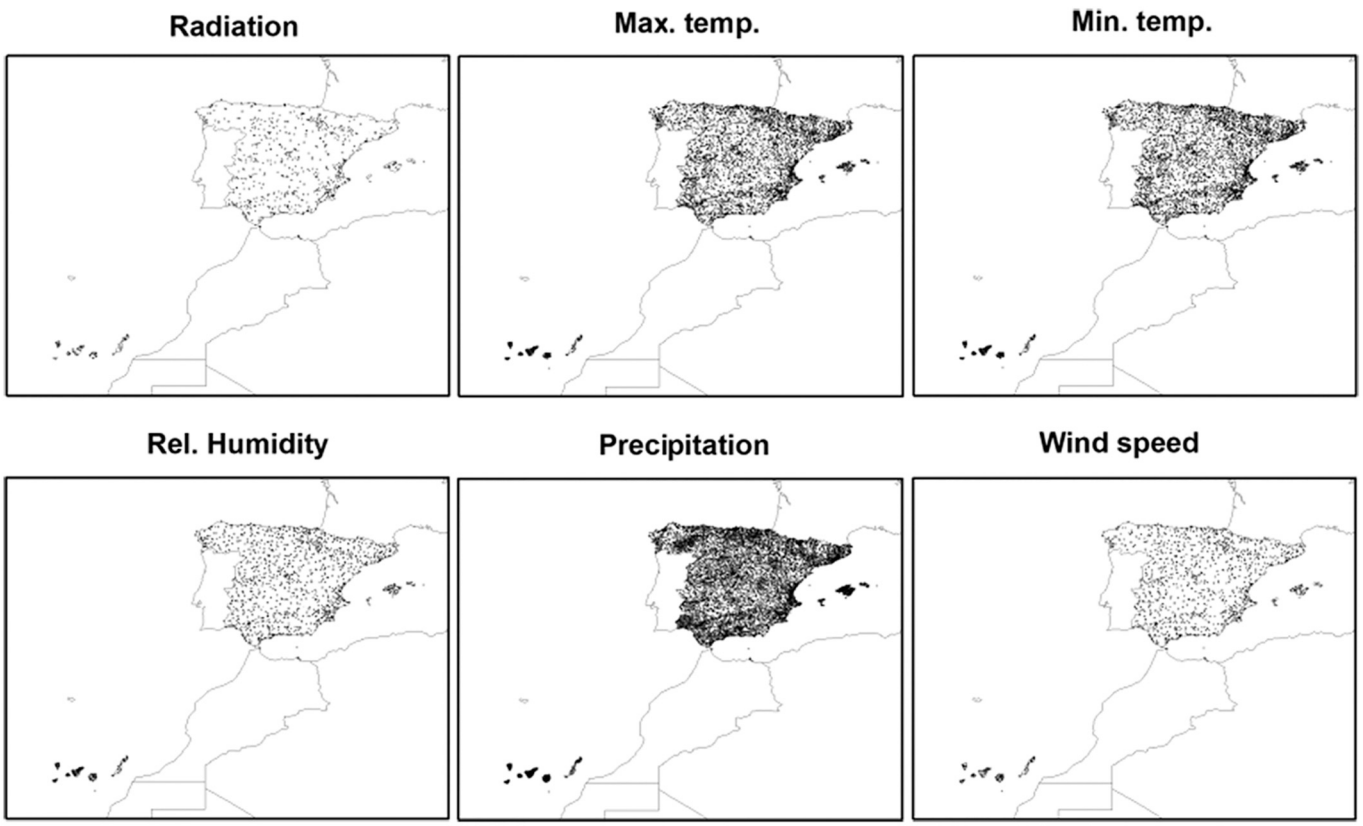

Fig. 1. Spatial distribution of meteorological data series available in Spain in the period 1961–2020, for different variables used in the drought monitor.

Table 1
Number of meteorological stations available for Spain for different meteorological variables, including the number of total stations and the number of stations that receive information in real-time (automated network).

	Total	Real-time
Solar Radiation	813	583
Max. Temp	5611	1238
Min. Temp.	5551	1238
Relative Hum.	1614	1237
Precipitation	11,139	1236
Wind speed	1436	1123

A preferred approach to drought monitoring is through impact metrics such as crop failure, livestock income given pasture loss, forest growth reduction, economic loss, etc. Nevertheless, drought impacts are challenging to quantify, and their data are usually lacking in real-time (Wilhite et al., 2007). For this reason, it is widespread to base drought monitoring systems on information sources that are available in near real-time and with high updating frequency. Examples of such data sources are climate-based metrics (Abatzoglou et al., 2017; Beguería et al., 2014; McRoberts and Nielsen-Gammon, 2012); numerical modelling of hydroclimatic variables, such as soil moisture, based on climate information (Lorenz et al., 2017; Sheffield et al., 2014; Zhang et al., 2017b; Zink et al., 2016); or remote sensing data (Adedeji et al., 2020; AghaKouchak et al., 2015; Atzberger, 2013; Yan et al., 2016).

Currently, there are several drought monitoring systems worldwide (Hao et al., 2017b; Heim and Brewer, 2012). Some of them have global (Beguería et al., 2014; Hao et al., 2014; Nijssen et al., 2014; Pozzi et al., 2013; Turco et al., 2020; Wood et al., 2015) or continental coverages (Abatzoglou et al., 2017; Fang et al., 2021; Sheffield et al., 2014). Such systems usually rely on low-spatial resolution data. Despite their unique capacity to provide a general picture of drought conditions over large areas, these systems offer excessively coarse information of little use for operative drought management on the national and local scales. Drought episodes frequently have a local character, so low-spatial resolution information does a lousy job of identifying their spatial extent, duration, and severity. Moreover, global and continental drought monitoring systems are usually based on low-spatial density information and rarely use all the existing hydroclimatic information sources. This makes necessary the development of high-spatial-resolution systems at national scales useful for operational decision-making (Abatzoglou et al., 2017; McRoberts and Nielsen-Gammon, 2012; Shah and Mishra, 2022; Zink et al., 2016).

An optimum approach to drought monitoring is through expert-based systems (Svoboda et al., 2001), in which different physical information (climate, hydrology, crop impacts, etcetera) is integrated, merged, interpreted, and distilled to provide a general picture of the drought severity. Such systems usually inform of the likely drought impacts at different levels (agricultural, hydrological, and ecological). Also, drought monitoring systems based on local and sectorial needs have been developed with the help of expert-based assessment (Ferguson et al., 2016). Nevertheless, most regions of the world lack the necessary resources to maintain this kind of system, which demands an extensive network of observers and, in general, strong personnel effort (Svoboda et al., 2002).

In any case, drought has a climatic origin in the vast majority of cases. Its major impacts are related to conditions characterised by reduced rainfall, which may be aggravated by the increase in atmospheric evaporative demand (Vicente-Serrano et al., 2020a). For these reasons, the development of drought monitoring systems based on real-time climatic information is a common approach. Climate variables are usually transformed into synthetic indices, the so-called drought indices (Heim, 2002; Mishra and Singh, 2010; Mukherjee et al., 2018), which typically show strong relationships with a large variety of drought impacts (Bachmair et al., 2018; Bachmair et al., 2015; Bachmair et al., 2016a, 2016b; Hannaford et al., 2015; Ji and Peters, 2003; Quiring and

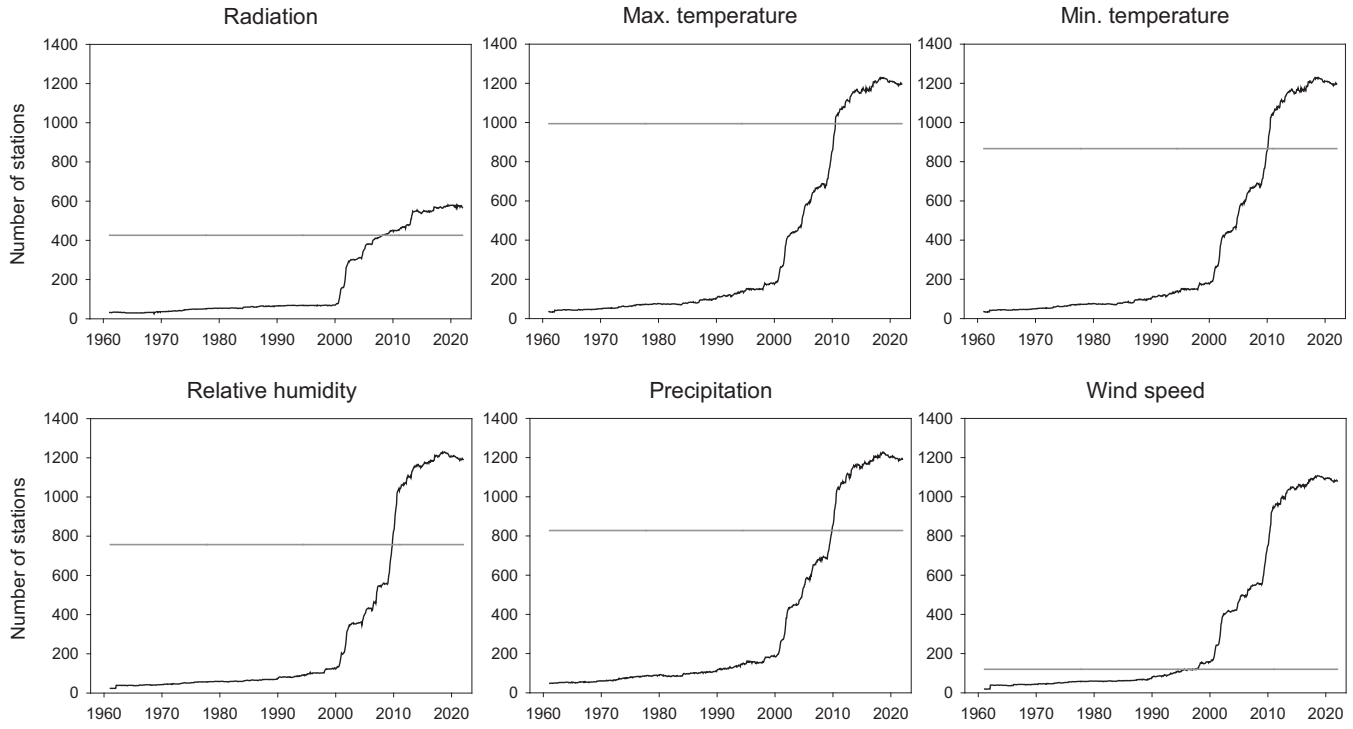

Fig. 2. Evolution of the number of meteorological stations that provide data in real-time for the different variables. Grey horizontal lines represent the number of stations in the final dataset after reconstruction of the stations.

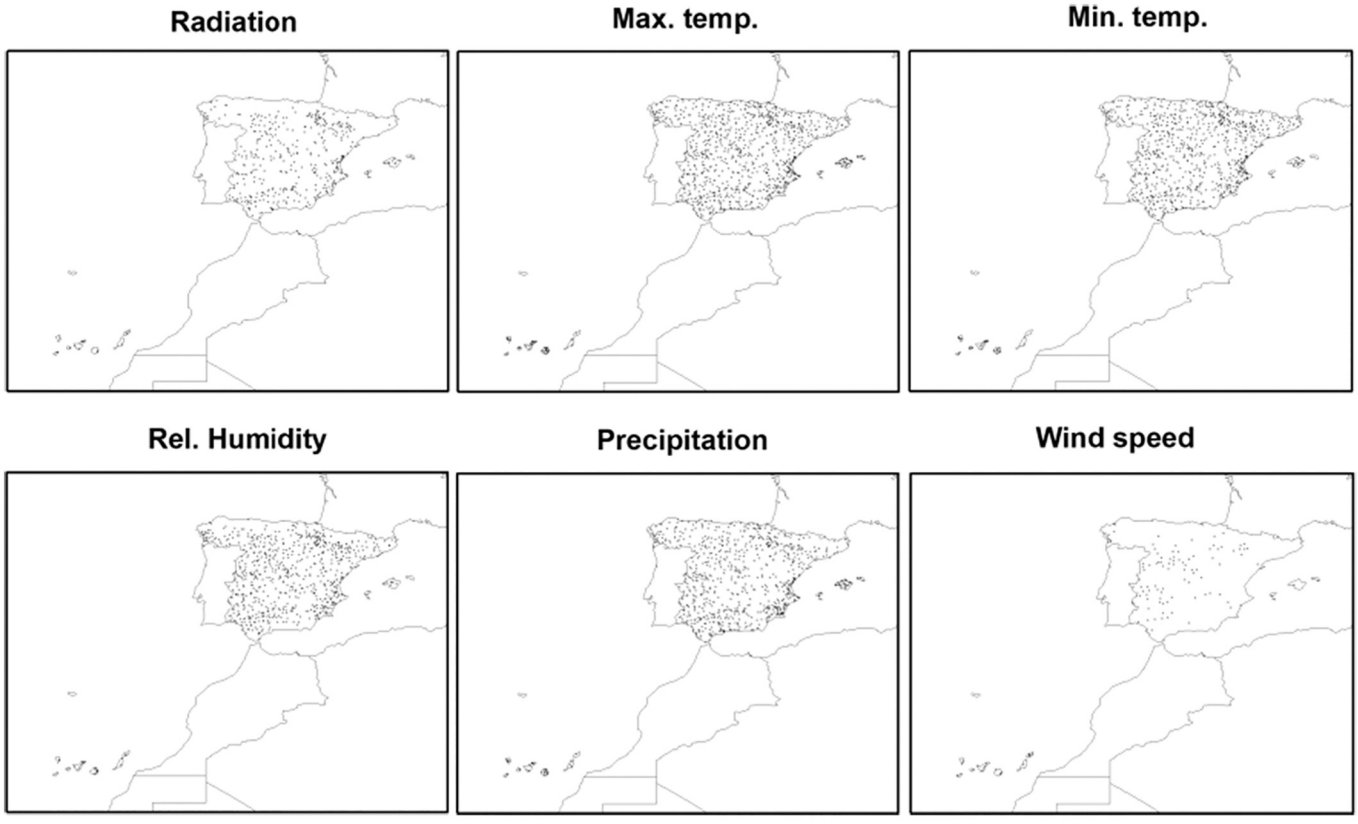

Fig. 3. Spatial distribution of the meteorological variables available in real-time to calculate the drought indices.

Table 2
Mean values of statistics comparing reconstructed and observed values of the variables in mainland Spain and the Balearic and Canary Islands: coefficient of determination (R^2), agreement index (D), mean absolute error (MAE) as a measure of goodness of fit; the mean error (ME).

		R^2	D	MAE	ME
Mainland Spain and Balearic	Sunshine dur. (hrs.)	0.92	0.98	0.68	0.02
	Max. Temp. (°C)	0.99	1	0.51	−0.01
	Min. Temp. (°C)	0.98	1	0.56	−0.04
	Dew Point Temp. (°C)	0.95	0.99	0.71	0.00
	Precipitation (mm)/corrected	0.83/ 0.88	0.94/ 0.96	5.57/ 4.11	−3.38/ −1.14
	Wind speed (km h-1)	0.77	0.94	0.28	0.01
Canary Islands	Sunshine dur. (hrs.)	078	0.94	0.73	0.02
	Max. Temp. (°C)	0.99	0.99	0.51	−0.01
	Min. Temp. (°C)	0.95	0.99	0.55	−0.03
	Dew Point Temp. (°C)	0.93	0.98	0.58	−0.05
	Precipitation (mm)	0.84	0.94	4.12	−3.22
	Wind speed (km h-1)	0.75	0.93	0.36	−0.03

Papakryiakou, 2003; Tian et al., 2018; Vicente-Serrano et al., 2012).

Despite the availability of real-time climate information thanks to automatic weather stations networks, the development of drought monitoring systems based on drought indices is still a complex task. Implementing a fully automatic drought monitoring system, which demands little maintenance effort, is necessary to solve several technical problems. This study describes the development of an automated Spanish drought monitoring system at high spatial resolution (1.1 × 1.1 km) and weekly frequency based on climatic drought indices. The system can determine a single point's drought severity even without direct climatic data, and it can also determine and monitor the development of drought episodes from a spatial perspective. A similar procedure to the one described here could be applied to other regions where real-time information is available from a network of automatic meteorological stations.

2. Data

Spain has a very dense network of weather stations. The historical network managed by the Spanish Meteorological Agency (AEMET) contains thousands of conventional meteorological stations and was reinforced by the installation of automatic weather stations (AWS) during the last two decades. In addition, the Ministry of Agriculture of Spain has developed a network of AWS over the previous two decades for agricultural purposes (SIAR). Fig. 1 shows the spatial distribution of the stations available for the different meteorological variables, including more than 10,000 precipitation stations and 5000 temperature stations, among other variables (Table 1). Precipitation is the primary variable determining drought severity (Tomas-Burguera et al., 2020), while the remaining variables allow for accurate quantification of the atmospheric evaporative demand (AED). The AED can be obtained using a physically-based approach, such as the FAO-56 Penman-Monteith equation (Pereira et al., 2015), and it is relevant mainly for assessing drought severity in a warming scenario (Dai et al., 2018; Vicente-Serrano et al., 2020a).

Despite the high density of stations of the whole network, the number of stations reporting at real-time is much smaller (Table 1). The automated network has been developed mainly during the last two decades. A few principal stations have been reporting real-time data using telephonic connections since the 1960s. Still, the vast majority of real-time stations are automatic stations installed since 2000 (Fig. 2).

We used all the meteorological information available during the period 1961–2020. However, for better understanding, the dataset can be split into two: on the one hand, the data from the automated network providing real-time meteorological data, required to update the drought monitor every week and keep the system operational; and, on the other hand, a long-term gridded dataset allowing comparing the current conditions with those of a sufficiently long period. However, all the data underwent a similar process of quality control and homogenisation, as described below.

Daily data of the different meteorological variables for the period 1961–2020 were quality-controlled according to a protocol that filters any suspicious data (Tomas Burguera et al., 2016). The data was afterwards summarised at a quasi-weekly temporal frequency. As drought indices are relative metrics and their calculation requires homogeneous periods, it was impossible to use calendar weeks as the reference periods since the first day of each year can fall on different days, which propagates throughout the entire year. The occurrence of leap years also increases the inhomogeneity of the weeks between years, adding difficulties to this comparison. For this reason, each month was divided into four artificial "weekly" periods: the first from the 1st to the 8th day, the second from the 9th to the 15th day, the third from the 16th to the 22nd day, and the fourth from the 23rd day to the end of the month. This approach enabled interannual comparison, which is essential for calculating drought indices. Once the "weekly" series were available, the fragmentary series were reconstructed using a gap-filling approach (Beguería et al., 2019) and finally homogenised. During homogenisation, the short-term series (< 25 years) were not considered candidate series to reconstruct. This was the case for most real-time (automated) meteorological stations since their data series are generally short. However, the described approach allowed obtaining long-term, gap-free and homogeneous time series starting in 1961. Finally, a gridded "weekly" dataset of the different meteorological variables based on long-term meteorological stations was generated at a spatial resolution of 1.1 × 1.1 km by Universal Kriging. A detailed description of the quality-control and homogenisation processes and the generation and validation of the gridded dataset set can be found in Vicente-Serrano et al. (2017a).

3. Methods

3.1. Processing, reconstruction and mapping of automatic meteorological series

Standardised drought indices are the preferred approach for quantifying drought severity (Heim, 2002; Mukherjee et al., 2018). In order to calculate standardised drought indices, data series of a certain length are required. This is so because standardisation of non-standard variables relies on parametric fitting and requires a minimum sample size to obtain reliable distribution parameters. Also, as the objective is to get a reliable characterisation of the climate of each site, the data series should be long enough not to be affected by internal climate variability (e.g. the dominance of dry or humid conditions during a short period). Usually, the minimum length of the series is set at 30 years (WMO, 2012), but some authors recommend at least 50 years (Guttman, 1999).

The need for long time series makes the calculation of drought indices from short automated network records impossible. As automated network data is fundamental for building a real-time monitoring system, it was necessary to undertake a data reconstruction to extend the length of the series. For this purpose, we used the long-term gridded data set described above.

We used two real-time networks: AEMET and SIAR. It is important to note that both network objectives are different. The AEMET network looks to maximise the climate representation of the stations, whereas the SIAR network focuses on evaluating crop water requirements. For this reason, SIAR stations are restricted to cultivated areas, while AEMET stations are located anywhere. We selected the available real-time

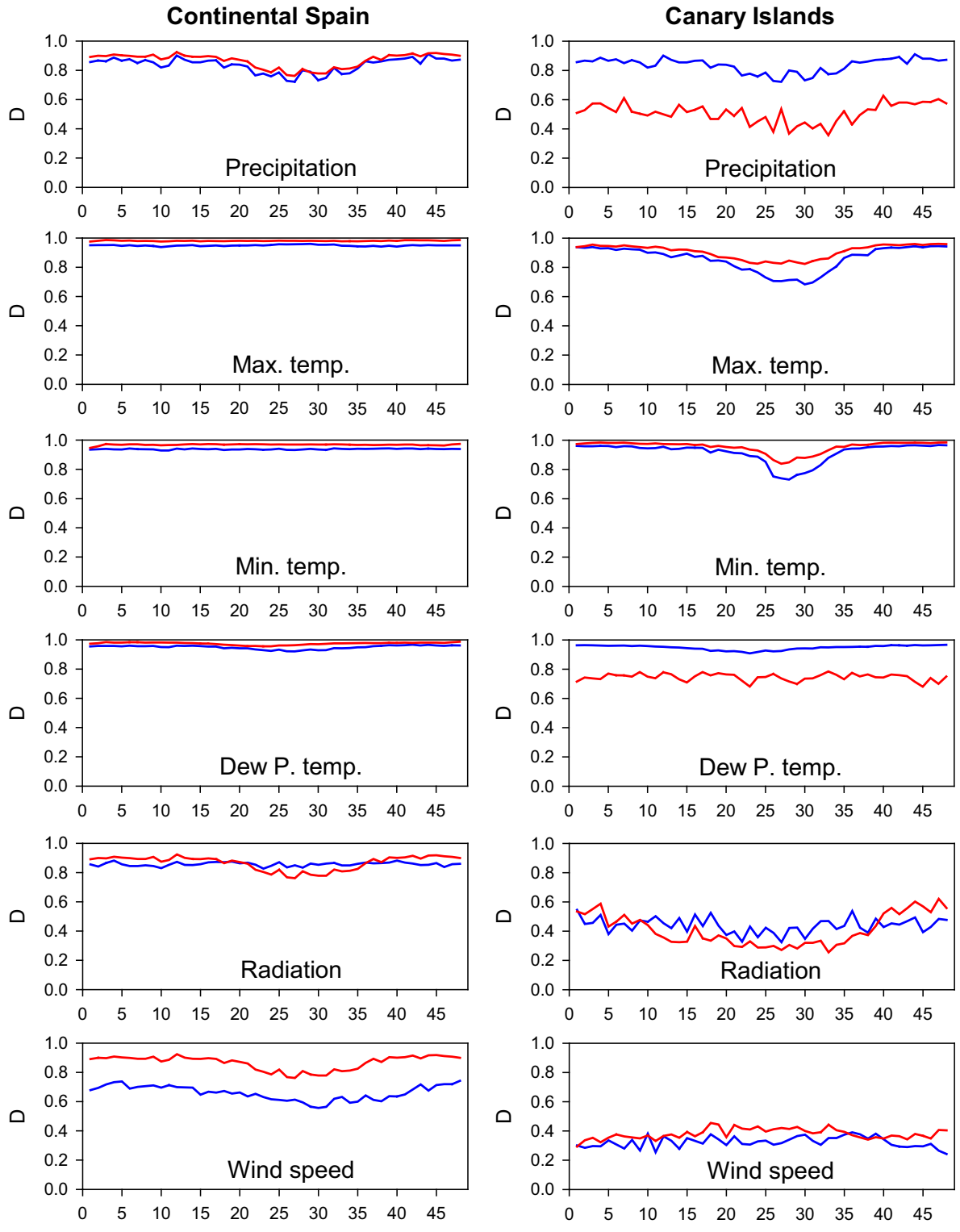

Fig. 4. Average D statistic for the different "weekly" periods of the year. Blue; gridded dataset obtained from the historical dataset obtained with all the series, Red: gridded dataset generated from the reconstructed real-time series from 1961 to 2020. (For interpretation of the references to colour in this figure legend, the reader is referred to the web version of this article.)

stations without operative problems during the year 2020, i.e. without gaps or anomalous values detected during the quality control (Tomas Burguera et al., 2016). Moreover, we discarded real-time stations with less than six years of data to have enough overlapping period with the long-term historical gridded variables to evaluate their quality. This pool of real-time stations was summarised into quasi weekly temporal frequency as we did with the gridded variables. We selected for reconstruction the series with a better agreement with the historical gridded variables. Therefore, we selected the series with Pearson's correlation coefficient above 0.8 and the refined Willmott's agreement index (D) (Willmott et al., 2012) above 0.83, 0.88, 0.88, 0.84, 0.87, and 0.78 for precipitation, Tmax, Tmin, dew point, sunshine duration, and wind

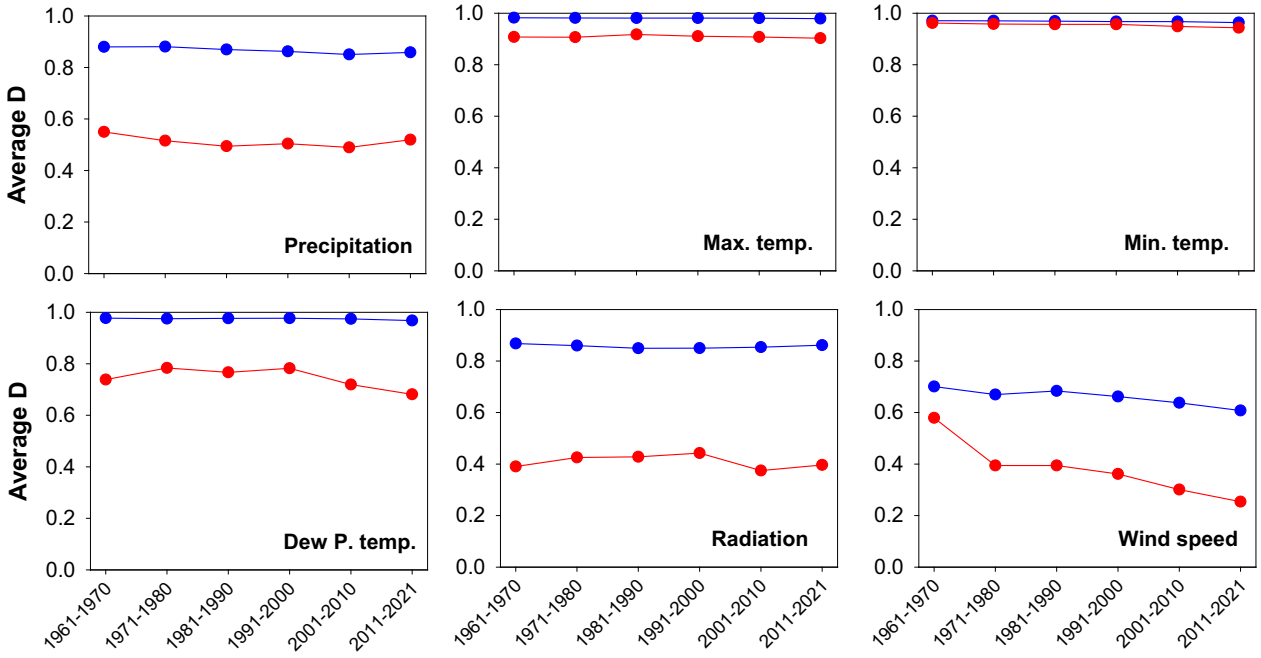

Fig. 5. Average decadal values of D for the different meteorological variables. Blue: Mainland Spain and the Balearic Islands, Red: Canary Islands. (For interpretation of the references to colour in this figure legend, the reader is referred to the web version of this article.)

speed, respectively. The agreement index (D) is a relative and bounded measure of model validity that scales with the magnitude of the variables, retains mean information and does not amplify outliers, allowing comparability independently of the different magnitudes between variables and seasons. D varies between 0 and 1, with the latter representing a perfect agreement between the observed and predicted data. The stations selected for the reconstruction process are shown in Fig. 3.

For each series selected for reconstruction, we generated a reference series following the gap-filling approach detailed in Beguería et al. (2019). We used the closest nine pixels of the historical gridded variables, weighed by the Pearson's correlation coefficient with the candidate series. Then we imputed the values of the reference series to the missing values of the real-time series. Finally, these series were homogenised by the Standard Normal Homogeneity Test (Alexandersson, 1986). The reference series provides values for the missing data and the observed ones, thus allowing us to assess the quality of the reconstruction process. Table 2 shows a set of evaluation statistics for each variable to evaluate the accuracy of the reconstruction process. These include the coefficient of determination (R^2), agreement index (D) and mean absolute error (MAE) as measures of goodness of fit and the mean error (ME) as a measure of bias.

All variables in continental Spain, the Balearic Islands, and the Canary Islands showed suitable goodness of fit values, with R^2 above 0.75 and D values above 0.93, being particularly high for sunshine duration, maximum, minimum, and dew point temperature. The MAE shows lower values for maximum than for minimum temperature, but in both cases, they are below 0.6 °C. The MAE of dew point temperature is also below 0.6 °C in the Canary Islands and 0.7 °C in mainland Spain and the Balearic Islands. The MAE values are also low for sunshine duration and wind speed. None of these variables (maximum, minimum, dew point temperatures, sunshine duration, and wind speed) show bias, with ME close to 0.

On the other hand, precipitation had an MAE of 5.5 mm and 4.1 mm for the continental and the Canary Islands, respectively. This MAE could be acceptable considering that it is an error for the sum of weekly precipitation. The ME, however, indicates signs of bias in the reconstruction of precipitation in mainland Spain and the Balearic Islands, with a value of −3.38 mm. This negative bias in the reconstructed part of the series generates a slight and artificial trend towards drier conditions that could affect the computation of SPI and SPEI. The artificial trend started around 2000 and increased in accordance with the availability of real-time data.

The origin of this bias is difficult to identify, but there are probably two important sources of error. One is the short length of the overlapping period between real-time stations and the gridded historical data at some stations. However, it is unclear how this would translate into bias and not just into general bad fitting (higher MAE). The other, more fundamental source of error is the differences in precipitation capture between automatic and manual stations. We must consider that the historical grid is vastly based on manual stations, while all the real-time stations are automatic. A growing number of studies report precipitation underestimation of automatic gauges with respect to their manual counterparts. In general, this underestimation is around 5–10%, but it is highly variable in time and space and therefore challenging to correct (Brandsma, 2014; Legates and DeLiberty, 1993; Talchabhadel et al., 2016; Valík et al., 2021). The leading cause of this underestimation is the different effects of systematic errors on manual and automatic stations, such as evaporation losses, wetting and wind (Sevruk et al., 2009). Fortunately, we can determine each real-time station's "natural" evolution in its corresponding pixel of the gridded dataset. So we used this information to correct the spurious trend in real-time reconstructions in the last decades. Therefore, we computed bias-correction coefficients for each real-time station and each week of the year based on the ratio between the mean precipitation of the gridded data and the real-time station in the same grid point for the period 2000–2020. This bias-correction factor is also applied weekly to the precipitation occurred after 2020 to avoid inhomogeneities. This correction reduced bias by around 60%, resulting in an ME of −1.14 mm per week, a value deemed acceptable for developing the monitoring system (Table 2).

Fig. 3 shows the spatial distribution of the real-time series available for the different meteorological variables after reconstruction. Except for wind speed, the variables had good spatial coverage and high spatial density in the critical meteorological variables of precipitation, air temperature, and dew point temperature. This is essential as in Spain, meteorological drought is mostly precipitation-driven (Noguera et al.,

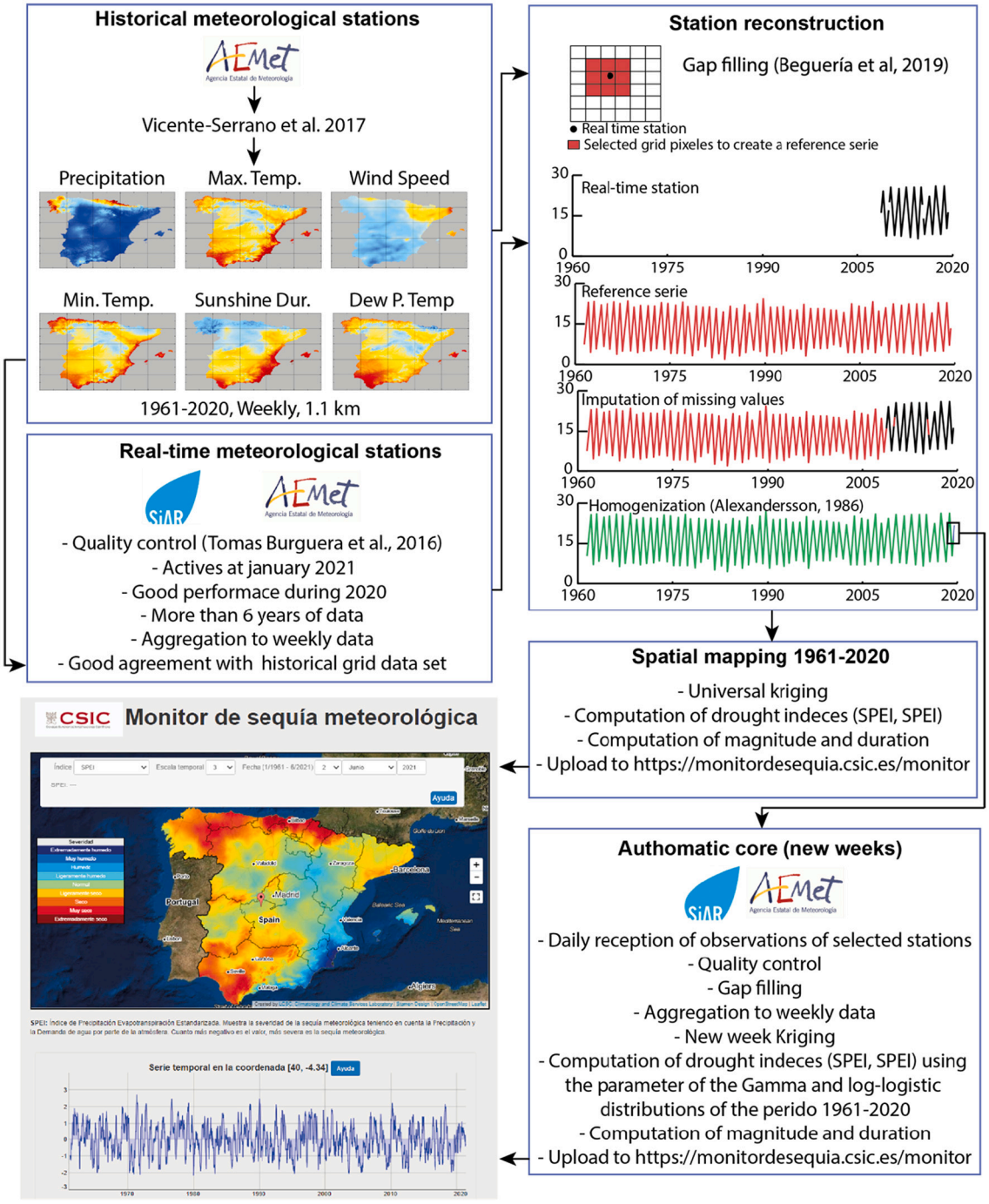

Fig. 6. Summary of the procedure for developing the drought monitoring system.

2021). However, the AED intensifies the severity of droughts caused by precipitation deficits, particularly in dry areas and in summer (Tomas-Burguera et al., 2020). The observed changes in AED over the last decades are driven mainly by changes in air temperature and relative humidity (Tomas-Burguera et al., 2020; Vicente-Serrano et al., 2014a; Vicente-Serrano et al., 2020a).

Once long-term automatic series were available for 1961–2020, they were interpolated at a spatial resolution of 1.1 × 1.1 km using Universal Kriging considering elevation, latitude, longitude and distance to the sea as co-variables. Validation was carried out using a leave-one-out jackknife approach (Phillips et al., 1992). Fig. 4 shows the average D statistic for the 48 "weekly" periods and the different variables. The plots allow comparing the mean D statistic from the historical gridded data using the available meteorological stations (in blue) and the reconstructed real-time meteorological stations (in red). The results are shown for both mainland Spain and the Canary Islands. In general, the average values of D are close to one, particularly for precipitation, air temperature, dew point temperature, and solar radiation. There are slight differences in the average D statistic between the grid dataset using all the available stations and the reconstructed real-time stations. The main exception is found in the Canary Islands, where the interpolation for precipitation and dew point temperature show more problems with datasets of automatic stations. The complex relief in the Canary Islands and the substantial differences in the climate and atmospheric influences among islands challenge establishing reliable interpolations using the limited availability of stations. In any case, an important issue is that the quality

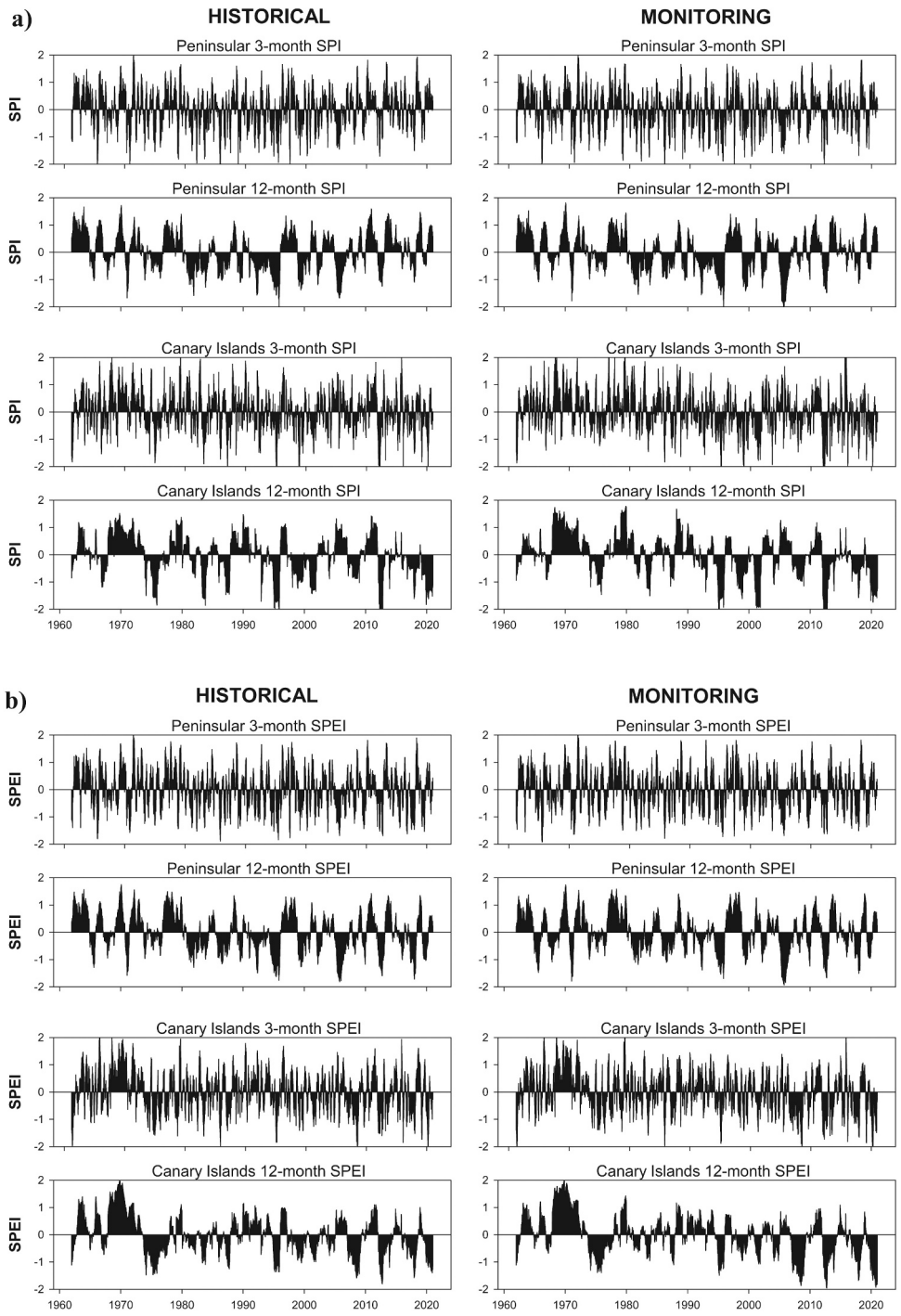

Fig. 7. a) Evolution of the average 3- and 12-month SPI in mainland Spain and the Balearic Islands and in the Canary Islands by means of the historical (left) and the monitoring (right) datasets, b) same as a) but with the SPEI.

of the historical gridded datasets does not show the same temporal bias as the D statistics, and they show comparable values across different decades (Fig. 5).

3.2. Computation of drought indices and automatic updating

Different drought monitoring systems are based exclusively on real-time precipitation data (McRoberts and Nielsen-Gammon, 2012). Relying only on precipitation simplifies the data availability problem vastly while maintaining the main operative characteristics of a drought monitoring system, as rainfall controls the availability of water resources, such as soil moisture, surface water, and groundwater (Alfieri et al., 2007; Bloomfield and Marchant, 2013; Folland et al., 2015; Lakshmi et al., 2018; Leuzinger and Körner, 2010; Lorenzo-Lacruz et al., 2017; Manning et al., 2018). Drought monitoring based on precipitation data commonly uses the Standardised Precipitation Index (SPI), which the World Meteorological Organization also recommends as the reference drought index for operative purposes (Hayes et al., 2011; WMO, 2012). This explains why the Spanish drought monitoring system includes the SPI as one of the primary metrics.

Nevertheless, global warming has increased the AED worldwide (Vicente-Serrano et al., 2020a; Wang et al., 2012), particularly in Spain

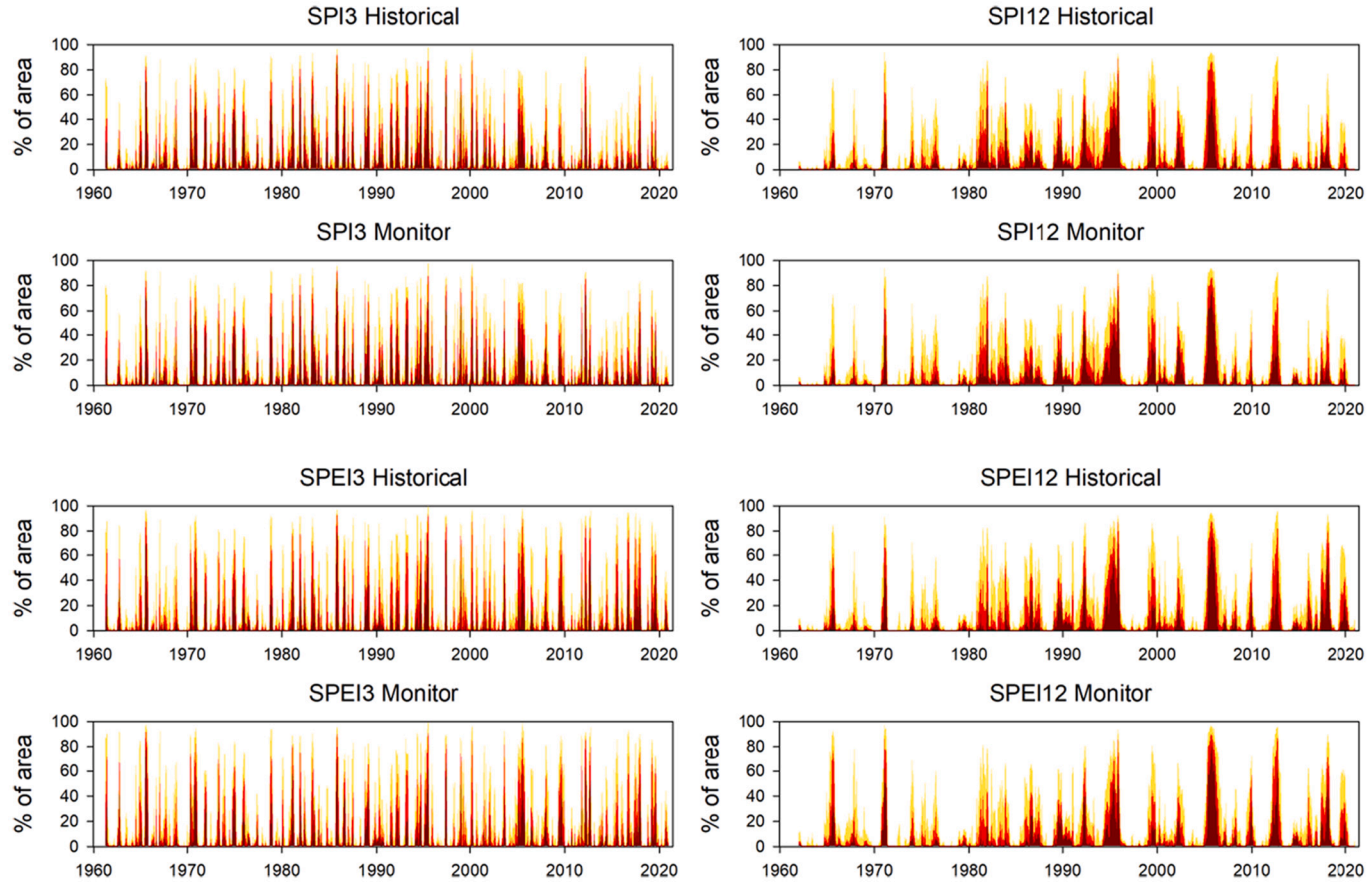

Fig. 8. Evolution of the surface area affected by different categories of drought severity (severe: red, moderate: orange, mild: yellow) in mainland Spain and the Balearic Islands with historical and monitoring datasets. (For interpretation of the references to colour in this figure legend, the reader is referred to the web version of this article.)

(Tomas-Burguera et al., 2020). Increasing AED reinforces the severity of drought events associated with precipitation deficits (Vicente-Serrano et al., 2014b). For this reason, the drought monitoring system also includes the Standardised Precipitation Evapotranspiration Index (SPEI). The SPEI is based on the difference between precipitation and the AED, which is standardised on different time scales (Beguería et al., 2014; Vicente-Serrano et al., 2010). The SPEI is sensitive to the AED mainly during periods of precipitation deficit or dry seasons, and particularly in areas characterised by low precipitation (Tomas-Burguera et al., 2020).

The information must be updated at a high frequency to make the drought monitoring system operational. This is especially relevant during the phases of development and reinforcement of drought, when knowing the evolution of the spatial extent and severity of the drought is helpful for water and land management. For this reason, the monitoring system would not be operative if, for each new "weekly" data available, a recalculation of the entire time series of the drought indices would be necessary to generate the new values for the last week. Moreover, considering a retrospective assessment, it is not helpful that the past values of the indices changed, although minimally, as a consequence of adding new data. To overcome this problem, we calculated the drought indices using a fixed reference period, from which the probability distribution parameters required to calculate the drought indices are computed. Then, the stored parameters are used to calculate the new indices as soon as new data becomes available (McRoberts and Nielsen-Gammon, 2012). This approach speeds up the process tremendously and makes it possible that the arrival of new data does not alter the previous values of the drought index. We used the reference period 1961–2020 to calculate the parameters of the Gamma and log-logistic distributions that are used to calculate the SPI and the SPEI, respectively (Stagge et al., 2015; Vicente-Serrano and Beguería, 2016). A set of parameters were obtained for each of the 48 periods of the year and for different time scales (1-, 3-, 6-, 9-, 12-, and 24-months).

Once the set of parameters was obtained for each grid cell and every weekly period, the system was ready to process new data. Every day, the meteorological data received from the Spanish Meteorological Agency and the Ministry of Agriculture is subject to automatic quality control (Tomas Burguera et al., 2016). Data gaps are filled at the end of the corresponding weekly period (Beguería et al., 2019), and weekly data aggregates are calculated. The data for the different variables are interpolated using Universal Kriging and the drought indices (SPI and SPEI) are calculated using the distribution parameters for the reference period. The maps are finally published on the web tool. The current temporal gap between new data availability and the publication of the drought indices maps is only two days. Fig. 6 summarises the procedure for developing a drought monitoring system that can serve as a guide for the reader.

3.3. Determination of areas under drought and drought duration

Although the values of the drought indices allow characterising the severity and spatial extent of drought conditions at any given moment, the characteristics of drought events such as their duration, spatial extent, and magnitude since the beginning of the drought are also of great concern. Therefore, we have included a method for identifying and tracking drought episodes since their onset. We considered a threshold equal to −1.28 of SPI/SPEI, corresponding to a return period of one in ten years, as the threshold value to determine the start of the drought event in a particular grid cell. Then, if the index values in the same grid

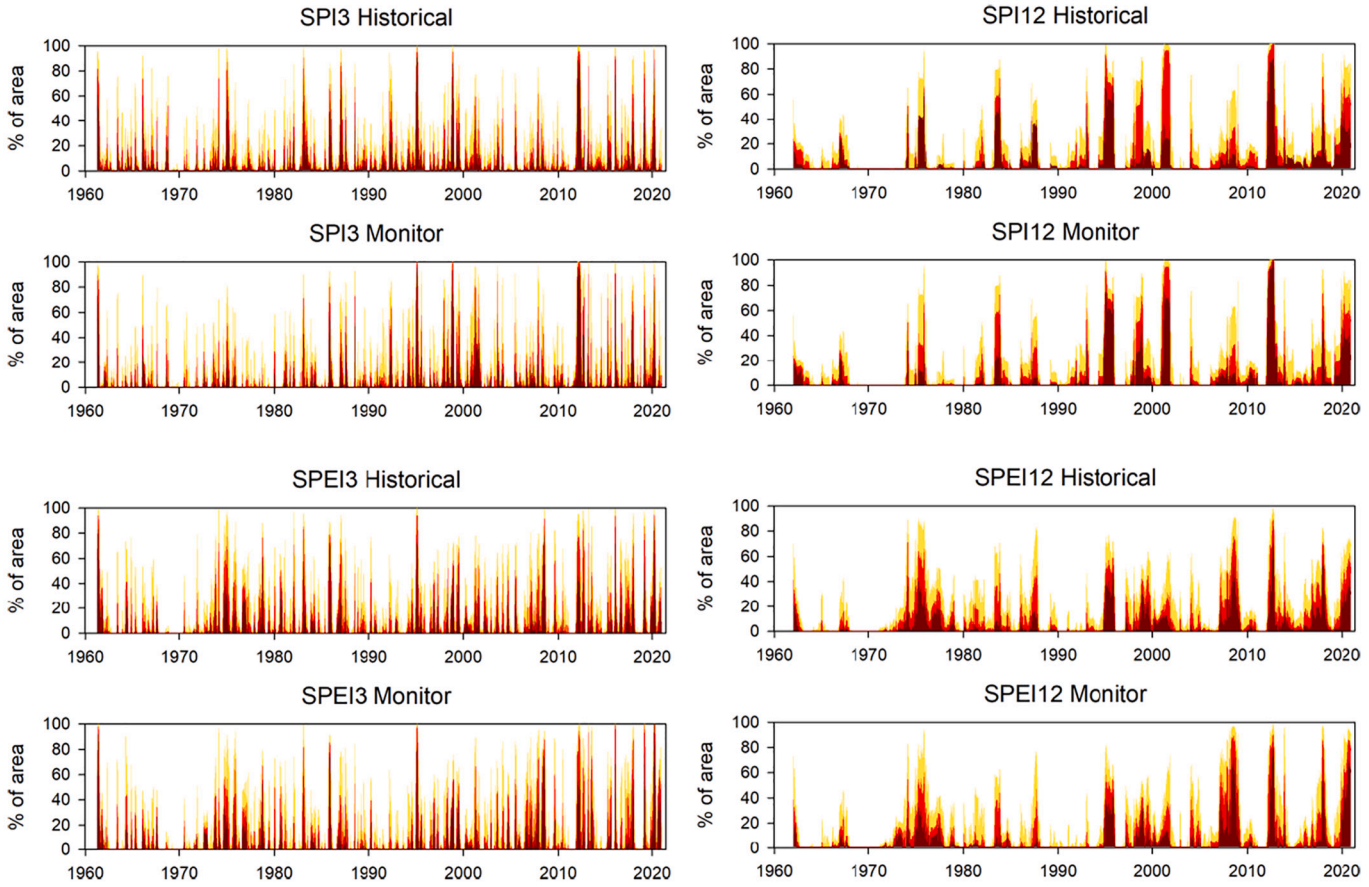

Fig. 9. Evolution of the surface area affected by different categories of drought severity (severe: red, moderate: orange, mild: yellow) in the Canary Islands with historical and monitoring datasets. (For interpretation of the references to colour in this figure legend, the reader is referred to the web version of this article.)

cell remain below this threshold, the system computes the episode's duration (in weeks) since its beginning and the cumulative drought magnitude (the sum of the drought index values). This allows visualising the spatial distribution of the total drought magnitude and duration since the beginning of the drought episode in each gridded cell, which constitutes an excellent way of assessing the spatial extent and evolution of a drought (Tallaksen et al., 1997; Van Loon, 2015).

3.4. Analysis

We compared the drought indices obtained from the time series of reconstructed automatic stations with the drought indices obtained from all the available meteorological stations, based on a carefully quality-controlled and homogenised dataset. Both datasets share common spatial and temporal resolutions, and the comparison considered the common period of 1961–2020.

First, we compared the spatial patterns of drought for each of the 2880 "weekly" periods. This allowed calculating Pearson's r correlation coefficients at each grid cell between the values of the drought indices from the historical dataset and the drought indices from the automatic stations dataset. To know if there is a spatial agreement in the identification of drought conditions, we classified the values of the indices as severe (SPI or SPEI < -1.65), moderate ($-1.65 <$ SPI or SPEI < -1.28), mild drought ($-1.28 <$ SPI or SPEI < -0.84) and no drought (SPI or SPEI > -0.84). A comparison between these categories was made by using a cross-tabulation and calculating the value of the coefficient of contingency (CC) in relation to the maximum CC in a matrix of 4×4 categories (De Luis et al., 2003). For each week, this approach allowed an assessment of the performance of drought conditions using real-time meteorological stations.

The third approach was temporal, and Pearson's r correlations and coefficients of contingency were calculated between both datasets for each time series. This allows identifying areas where there is more or less agreement between both datasets when determining the temporal evolution of the drought indices and the different categories of drought severity. Finally, we also calculated the relationship between the evolution of the area affected by severe, moderate and mild droughts. The comparison was based on both SPI and SPEI on 3- and 12-month time scales, and it was developed separately using the datasets of continental Spain and the Canary Islands.

4. Results

Fig. 7 compares the average drought evolution over Spain with the historical data set using all the available stations and the dataset from the reconstructed meteorological stations. The average series shows strong agreement between the indices obtained from the historical dataset and the indices from the monitoring dataset. In particular, for the mainland Spain and the Balearic Islands datasets, the correlation between the SPI series and the SPEI series is >0.99, independently of the drought time scale. The agreement is lower in the Canary Islands, but correlations are still very high (0.92–0.93 for the SPI series and 0.96 for the SPEI series). The temporal patterns of the main drought episodes and the drought severity are well recorded in the monitoring dataset.

There is also a high agreement between the area affected by different categories of drought severity, both in the mainland Spain and the Balearic Islands (Fig. 8) and in the Canary Islands (Fig. 9). Thus, the Pearson's r correlations are higher than 0.97 in all of the cases. The spatial extent of the drought episodes identified by the drought monitoring system closely resembles those from the historical dataset

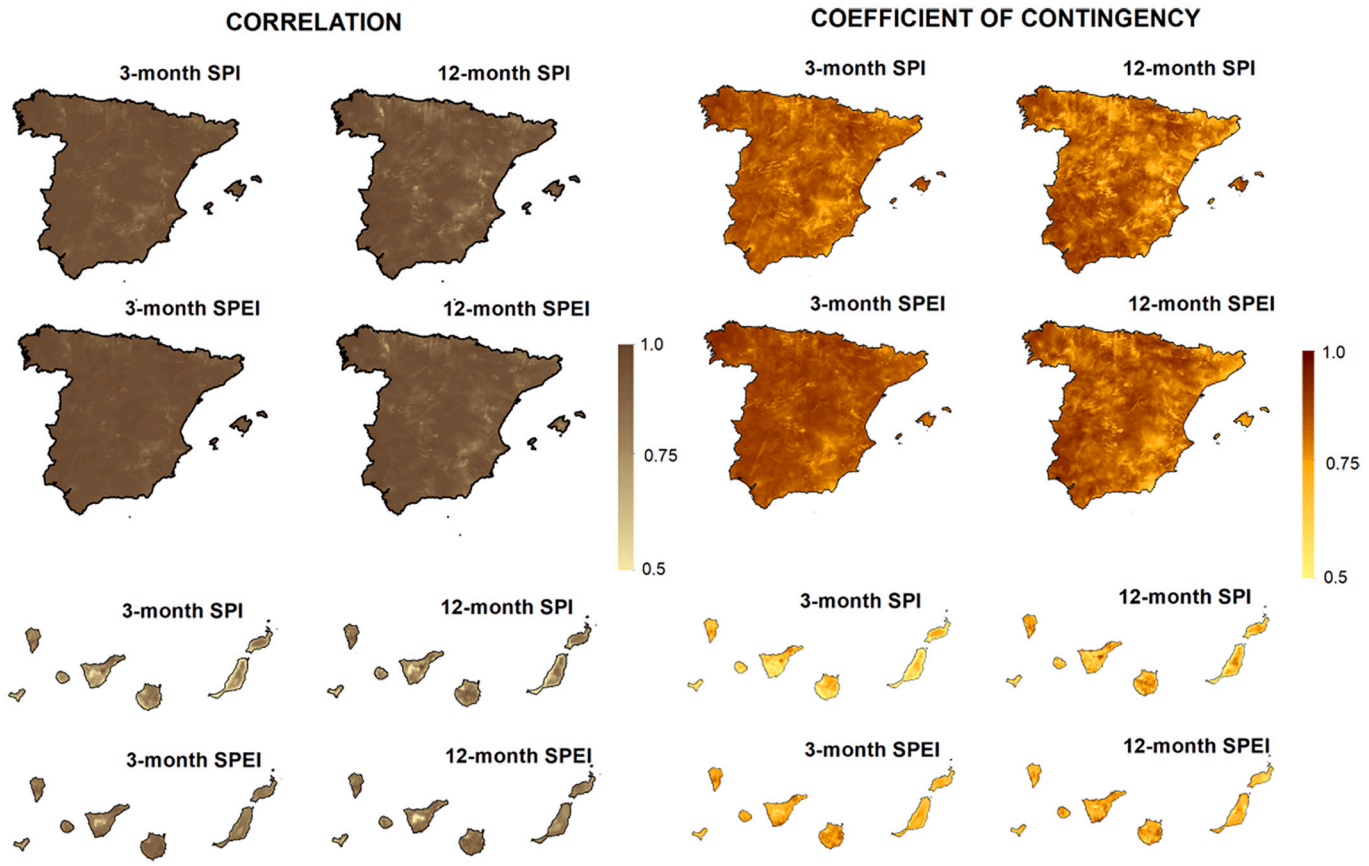

Fig. 10. Left: Spatial distribution of Pearson's r correlations between the SPI and SPEI series of historical and monitoring datasets in mainland Spain and the Balearic Islands (top) and the Canary Islands (bottom). Right: Same as left, but spatial distribution of the coefficients of contingency.

generated by the totality of the available meteorological stations. This result validates the monitoring system not only in its capacity to identify the spatial and temporal patterns of drought but also the main categories of drought severity. Thus, both large-scale droughts affecting most of the region and regional drought events that affected smaller parts were very well recorded by the drought monitoring system.

The spatial patterns of temporal correlation between the SPI and SPEI of both datasets show that in most of mainland Spain and the Balearic Islands, correlations and coefficients of contingency are very high. In the Canary Islands, the agreement between both datasets is lower, and it is higher in the SPEI than in the SPI. There are no spatial patterns that may characterise areas with lower relationships (Fig. 10). These results reinforce that, independently of the region under analysis, the relationship between both datasets is strong. The drought indices from the monitor dataset allow quasi-perfect identification of the drought evolution in relation to the historical dataset characterised by a higher number of stations.

Nevertheless, it is not only the high temporal agreement between the historical and the monitoring datasets, but the high spatial agreement between both datasets as well. Fig. 11 shows box plots with Pearson's r correlations between the spatial distribution of the SPI and SPEI values during the dry periods in which at least 30% of the territory was affected by moderate droughts. It also shows the Contingency Coefficients, which relate to the spatial agreement between the different categories of drought severity. In mainland Spain and the Balearic Islands, the box plots demonstrate that the spatial patterns of the drought indices and the distribution of the drought severity categories identified with the monitoring dataset show a strong resemblance with the spatial patterns identified with the high-quality historical dataset. There are few differences between SPI and SPEI, and the agreement tends to be slightly better at the 3-month than at the 12-month time scale. Given the strong spatial complexity of the relief and the climate influences in Spain, the spatial agreement between both datasets is lower. Given the difficulties in mapping precipitation in the region, this is more evident with the SPI. Nevertheless, the SPEI provides better spatial agreement, suggesting that including the AED in the calculations reduces the spatial uncertainty when developing the monitoring dataset.

The close relationship between the drought indices obtained from the historical and the monitoring datasets is illustrated in Figs. 12 and 13. As illustrated, two examples of the spatiotemporal evolution of the 12-month SPEI during the drought events that affected Spain in 2001 and 2012 are presented. Both drought episodes were very different in terms of drought spatial extent and severity. In 2001, a drought episode started in the North and Western Iberian Peninsula in December, and it intensified and expanded to other areas in January and February. The severity, spatial extent, and temporal evolution of the drought conditions identified in the historical dataset are very well represented by the monitoring dataset. The drought episode of 2012 affected most of Spain. This widespread expansion of drought conditions was well identified by the drought monitoring dataset. The existing spatial differences during the months of this drought episode were well recorded.

The Spanish Drought Monitoring System (*Monitor de Sequía Meteorológica de España*) is available at https://monitordesequia.csic.es/monitor. The web tool has two main components. On the one hand, the

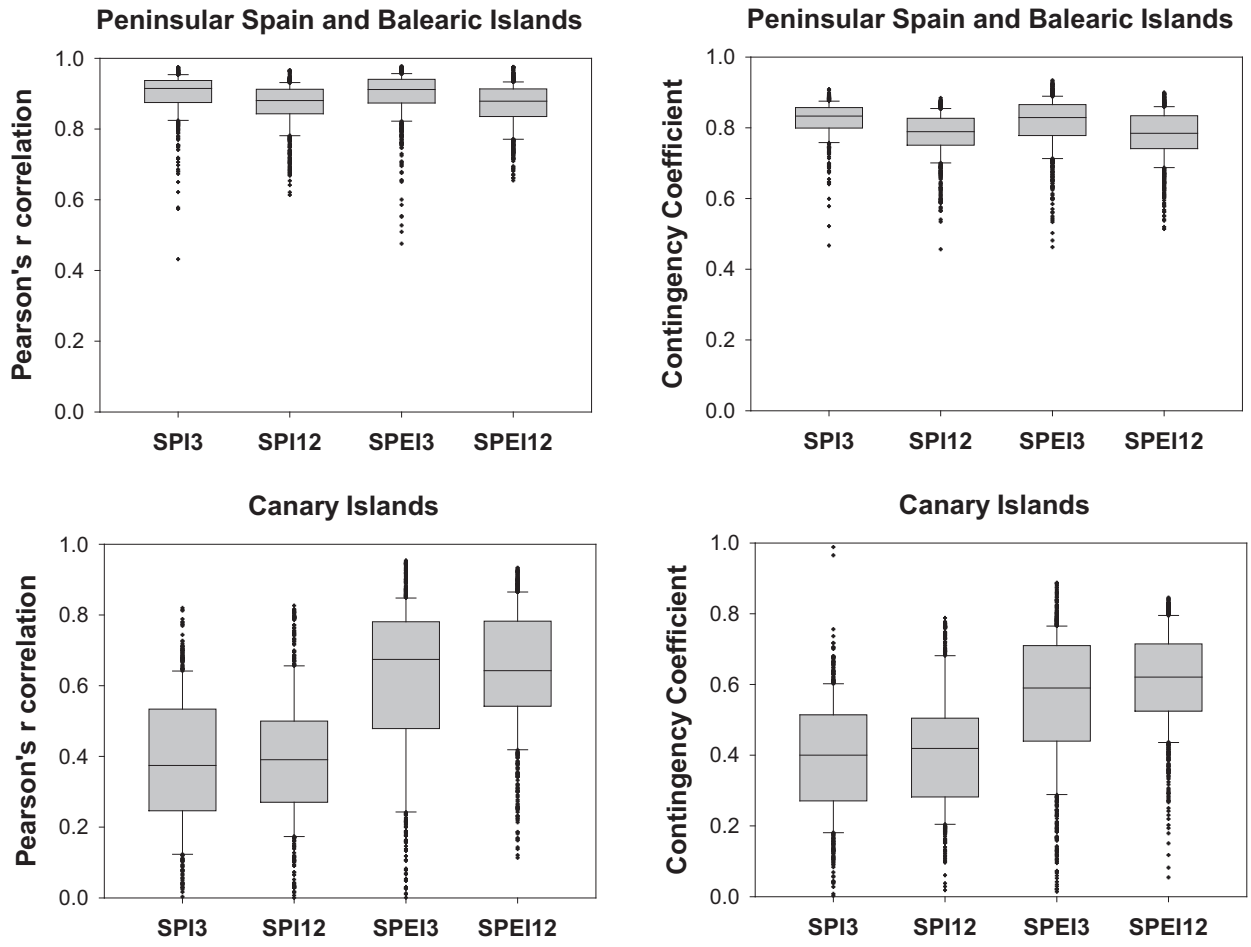

Fig. 11. Left: Box-plots showing the values of Pearson's r correlations between SPI and SPEI series obtained from historical and monitoring datasets in mainland Spain and the Balearic Islands (Top) and the Canary Islands (Bottom). Right: Box-plots showing the coefficients of contingency between different categories of drought (i.e. severe, moderate and mild) calculated from SPI and SPEI series obtained from historical and monitoring datasets in mainland Spain and the Balearic Islands (Top) and the Canary Islands (Bottom).

web tool includes an interactive map box in which the user may select the drought index (SPI, SPEI, and the drought duration and magnitude according to the drought index), the time scale of the drought index (1, 3, 6, 12 or 24 months) and the date (Fig. 14). The home map in the web tool is always the latest week available, but users may also visualise all the weekly maps from 1961 to the present. This can be useful for comparing the spatial extent and severity of a particular drought event and determining how drought severity and spatial extent evolve over time. Users may apply zooms to the maps, consult the values by the cursor location, and visualise the system over the whole screen. The second part of the web tool allows the selection of a point on the map, and then, automatically, a plot is displayed with the time series of the selected drought index at the chosen grid cell. This time series changes when different drought indices or time scales are chosen. The plot is also interactive as the user may consult the index values at any week of the time series and zoom to specific periods. Finally, there is a button to download the time series of the selected coordinates. The data is downloaded in text format as comma-separated values (csv), including all the data series (two indices, six-time scales and drought duration and intensity).

The web tool allows monitoring the development of a drought episode, determining the drought severity and spatial extent changes. This is illustrated by the last intense drought event that affected continental Spain in 2017 (Fig. 15). On the time scale of 12-months, this drought event started in May in the north of Spain, and it expanded to the west and centre of Spain over the following weeks. The maps of the 12-month SPEI illustrate the development of the drought event spatially and how the drought conditions intensified over several regions of Spain. At the same time, the information about the drought duration since the beginning of the event allows determining those areas that are being affected by drought conditions during more prolonged periods, which is helpful in determining where the most substantial impacts can be recorded. In this particular event, at the end of May 2017, large areas of northern Spain were affected by drought for more than ten weeks.

5. Discussion and conclusions

This study has shown a procedure for developing an automatic drought monitoring system based on meteorological drought indices useful for assessing drought severity at a high temporal frequency and high spatial resolution. This system can improve drought preparedness across Spain in an operative, automatic and non-expensive way. This approach is necessary nowadays to mitigate drought impacts and establish better adaptation measures (Wilhite, 2002).

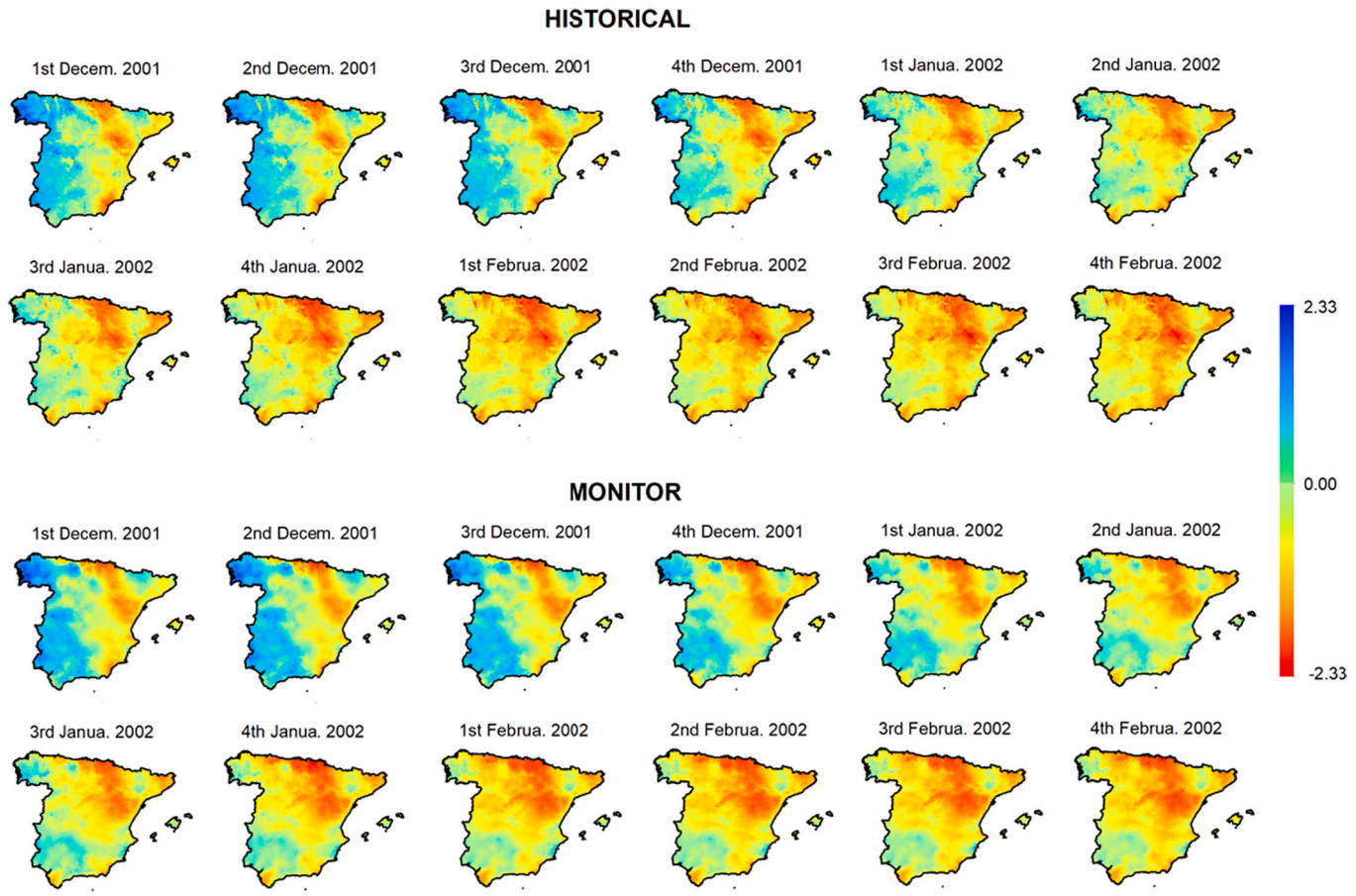

Fig. 12. Spatio-temporal evolution of the weekly 12-month SPEI between December 2001 and February 2002 with the historical data set and the drought monitoring dataset.

5.1. The use of drought indices in drought monitoring services

The use of drought indices for assessing drought severity has been criticised (Berg and Sheffield, 2018; Seneviratne and Ciais, 2017). Some authors have deemed drought indices an inferior approach as compared to the outputs from earth-surface models, sometimes coupled with biophysical models, which try to reproduce the evolution of drought severity based on simulated soil moisture and runoff (Cammalleri et al., 2015; Fang et al., 2021; Nijssen et al., 2014). These variables would be more directly related to drought-related impacts due to shortages in water availability to supply the water needs of natural vegetation, crops, and human societies in general. Nevertheless, soil moisture and runoff models still show substantial uncertainties. From a hydrological standpoint, models tend to fail in the reproduction of the severity and duration of low-flow periods (Tallaksen and Stahl, 2014), and studies showing the relationship between soil moisture observations and simulations show low general agreement (Ford and Quiring, 2019; Yuan and Quiring, 2017). For these reasons, although climatic drought indices are indirect metrics of soil moisture and water availability, they are strongly correlated with usable water sources like soil moisture, streamflow, and reservoir storage (Bloomfield et al., 2018; Burke, 2011; López-Moreno et al., 2013; Lorenzo-Lacruz et al., 2017; Scaini et al., 2015; Wang et al., 2016; Yuan et al., 2020). Therefore, they often exhibit a higher correlation with observations of these variables than the outputs from earth-surface models (Yuan et al., 2020).

Moreover, from a plant perspective, it is necessary to stress that soil water availability is not the unique driver that controls plant water stress, with implications for assessing agricultural and ecological drought conditions. AED increases plant stress, particularly during low soil water availability (Vicente-Serrano et al., 2020a, 2020b). Increased AED, combined with low water availability, enhances plant mortality risk (Grossiord et al., 2020; McDowell and Allen, 2015; Williams et al., 2013), but it also affects plant physiology by controlling stomatal closure and carbon uptake (Breshears et al., 2013; Eamus et al., 2013). These plant stress conditions are not considered in drought monitoring metrics that do not consider anomalies in the AED. On the contrary, drought indices like the SPEI account for both necessary elements: water supply through precipitation and atmospheric demand. Moreover, the meteorological drought indices used in the Spanish drought monitoring system are obtained from a high density of real-time observations, and spatial interpolation shows high quality demonstrated by accuracy statistics, which confers high reliability for assessing drought conditions.

Previous studies analysing the performance of the drought indices used here have demonstrated their utility to monitor particularly severe drought events as in 1996 in the US (Hayes et al., 1999), 2012–2016 in California (Abatzoglou et al., 2017), and in 2017 in western Europe (García-Herrera et al., 2019). This is due to the strong relationship between the drought severity quantified with the climatic drought indices and various drought impacts (Bachmair et al., 2016a, 2016b; Wang et al., 2020). Thus, a strong relationship between crop yields and SPI and SPEI has been found in different regions of the world (Páscoa et al., 2017; Potopová et al., 2016). Vegetation activity, leaf area and

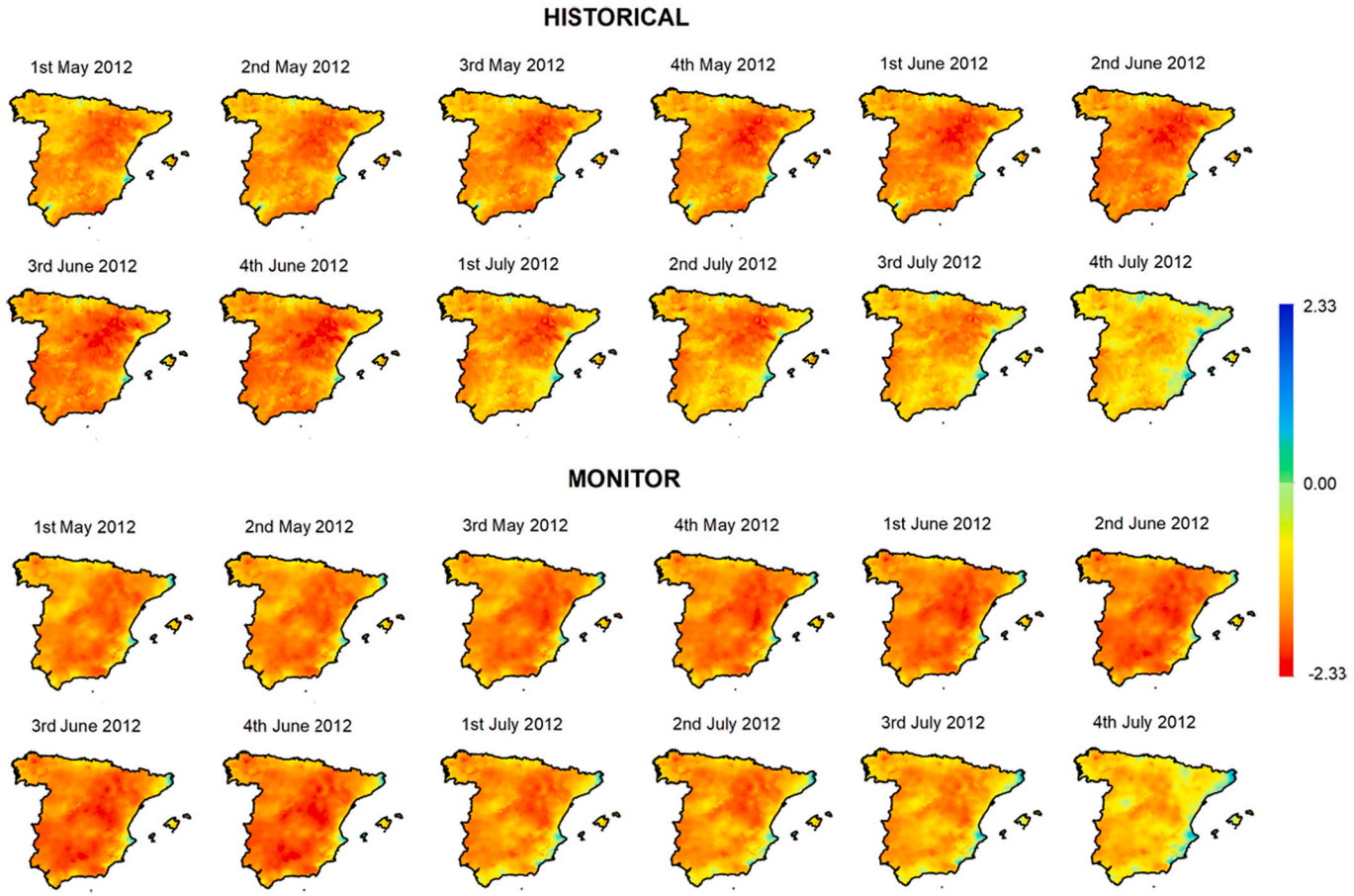

Fig. 13. Spatio-temporal evolution of the weekly 12-month SPEI between May 2012 and July 2012 with the historical data set and the drought monitoring dataset.

secondary tree growth are also closely related to these drought indices (Bachmair et al., 2018; Bhuyan-Erhardt et al., 2019; Zhang et al., 2017a) but also streamflow variability (Abatzoglou et al., 2014; Lorenzo-Lacruz et al., 2013), reservoir storages (Vicente-Serrano and López-Moreno, 2005) and groundwater (Bloomfield et al., 2018; Lorenzo-Lacruz et al., 2017). In particular, in Spain, different studies have shown that drought-related impacts are well identified by the SPI and the SPEI, including forest growth (Peña-Gallardo et al., 2018; Vicente-Serrano, 2021); vegetation activity (Gouveia et al., 2016; Gouveia et al., 2012; Vicente-Serrano et al., 2019); crop yields (Páscoa et al., 2017; Peña-Gallardo et al., 2019; Ribeiro et al., 2019); streamflow (López-Moreno et al., 2013; Lorenzo-Lacruz et al., 2013; Lorenzo-Lacruz et al., 2010; Vicente-Serrano et al., 2014b); reservoir storage (Lorenzo-Lacruz et al., 2010; Vicente-Serrano et al., 2017b; Vicente-Serrano, 2021); or groundwater (Lorenzo-Lacruz et al., 2017). Notably, the SPEI has shown a better performance to identify drought-related impacts than the SPI in environmental, hydrological and agricultural systems (Peña-Gallardo et al., 2019; Peña-Gallardo et al., 2018; Vicente-Serrano et al., 2014b), suggesting a role of the AED to intensify drought severity. All these previous results suggest that the assessment and monitoring of drought conditions based on these indices are highly operative to identify different drought types and their related impacts. The use of varying time scales of the two indices used here includes the necessary flexibility to assess different drought types considering the diversity of geographic, climatic, environmental and hydrological characteristics. For these reasons, the drought monitoring system developed for Spain is valuable for assessing meteorological drought conditions and determining the possible propagation of the drought impacts throughout the hydrological cycle and across different environmental systems and socio-economic sectors.

5.2. *Challenges to develop drought monitoring systems*

The main challenge in developing the Spanish drought monitoring system was to generate a robust dataset based on short series obtained from automatic meteorological stations with sufficient length to calculate the climatic drought indices with the necessary robustness. We have demonstrated that the application of techniques for reconstruction of climate series (Beguería et al., 2019) based on the whole number of available historical meteorological stations has allowed us to obtain homogeneous long-term series that extend to the short-term available automatic stations and that would enable us to develop high spatial resolution gridded data sets affected by minor errors. This is an essential task before making the system operative, as long-term datasets allow calculating the necessary distribution parameters to calculate the drought indices in real-time automatically. Moreover, the web tool developed needed to be interactive and intuitive, with several functionalities and options, but always well explained to the users. Intuitive systems are essential to make the information accessible to various stakeholders and end-users (Noel et al., 2020; Sheffield et al., 2014) to make the system usable independently of the training on drought monitoring.

The procedure described in this article could be easily implemented

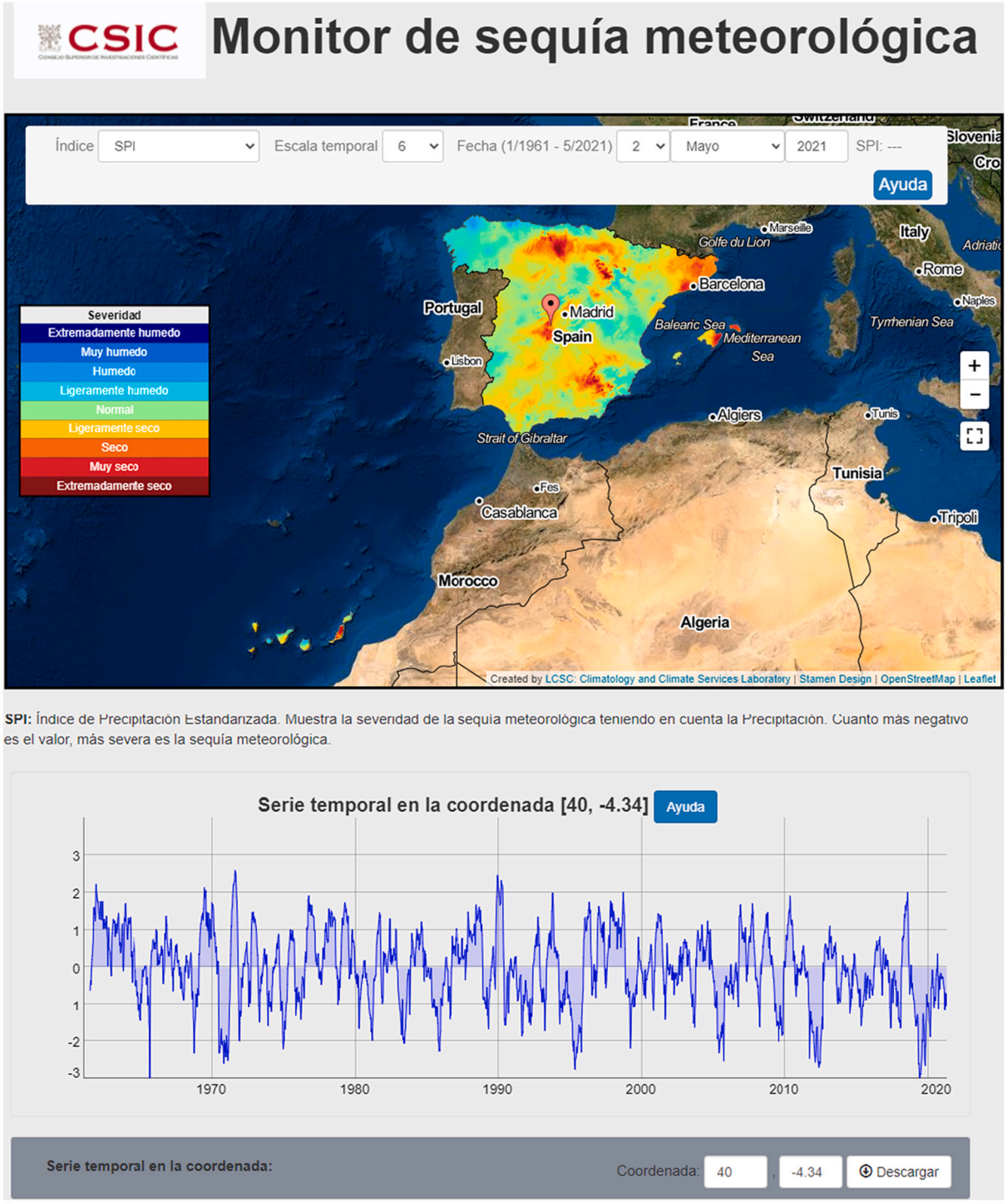

Fig. 14. Web-tool for the drought monitoring system in Spain.

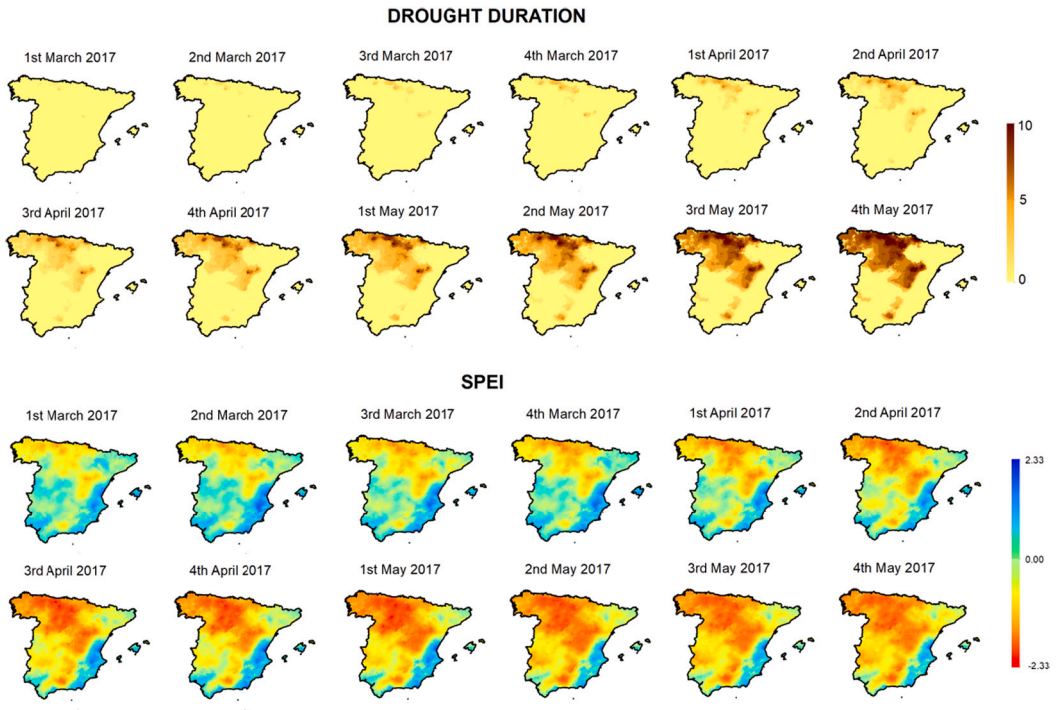

Fig. 15. Spatio-temporal evolution of the 12-month SPEI and the duration of the drought event (in weeks) at the same temporal scale since the beginning of the event between March 2017 and May 2017.

in other regions where a network of automatic meteorological stations exists together with a historical dataset of meteorological stations with a length of at least 30–40 years. This approach has been stressed by other studies that developed drought automatic monitoring tools and software packages (Hao et al., 2017a; Mol et al., 2017). It has the potential to create a high-spatial and temporal resolution drought monitoring system at a low cost, with minor maintenance, and automatic updating. In addition, it has the flexibility to assess drought severity across different environmental systems and socio-economic sectors, providing similar or better performance than costly systems in which the primary data inputs are from a network of observers or satellite systems. Future development tasks should include a quantitative sectorial evaluation of the performance of the climatic drought indices and time scales to relate the quantitative values to specific drought types spatially and to develop a synthetic metric that may also be generated automatically for each drought type (agricultural, ecological, and hydrological) (Hannaford et al., 2015), to contribute to better and earlier identification of drought impacts and more efficient mitigation.

Declaration of Competing Interest

The authors declare that they have no known competing financial interests or personal relationships that could have appeared to influence the work reported in this paper.

Acknowledgements

This work was supported by projects PCI2019-103631 financed by the Spanish Ministry of Science and Technology and FEDER and CROSSDRO project funded by AXIS (Assessment of Cross (X) - sectoral climate Impacts and pathways for Sustainable transformation), JPI-Climate co-funded call of the European Commission.

References

Abatzoglou, J.T., Barbero, R., Wolf, J.W., Holden, Z.A., Abatzoglou, J.T., Barbero, R., Wolf, J.W., Holden, Z.A., 2014. Tracking interannual streamflow variability with drought indices in the U.S. Pacific Northwest. J. Hydrometeorol. 15, 1900–1912. https://doi.org/10.1175/JHM-D-13-0167.1.

Abatzoglou, J.T., McEvoy, D.J., Redmond, K.T., 2017. The west wide drought tracker: drought monitoring at fine spatial scales. Bull. Am. Meteorol. Soc. 98, 1815–1820. https://doi.org/10.1175/BAMS-D-16-0193.1.

Adedeji, O., Olusola, A., James, G., Shaba, H.A., Orimoloye, I.R., Singh, S.K., Adelabu, S., 2020. Early warning systems development for agricultural drought assessment in Nigeria. Environ. Monit. Assess. 192, 798. https://doi.org/10.1007/s10661-020-08730-3.

AghaKouchak, A., Farahmand, A., Melton, F.S., Teixeira, J., Anderson, M.C., Wardlow, B. D., Hain, C.R., 2015. Remote sensing of drought: Progress, challenges and opportunities. Rev. Geophys. 53, 452–480. https://doi.org/10.1002/2014RG000456.

Alexandersson, H., 1986. A homogeneity test applied to precipitation data. J. Climatol. 6, 661–675. https://doi.org/10.1002/joc.3370060607.

Alfieri, J.G., Blanken, P.D., Yates, D.N., Steffen, K., 2007. Variability in the environmental factors driving evapotranspiration from a grazed rangeland during severe drought conditions. J. Hydrometeorol. 8, 207–220. https://doi.org/10.1175/JHM569.1.

Atzberger, C., 2013. Advances in remote sensing of agriculture: context description, existing operational monitoring systems and major information needs. Remote Sens. 5, 949–981. https://doi.org/10.3390/rs5020949.

Bachmair, S., Kohn, I., Stahl, K., 2015. Exploring the link between drought indicators and impacts. Nat. Hazards Earth Syst. Sci. 15, 1381–1397. https://doi.org/10.5194/nhess-15-1381-2015.

Bachmair, Sophie, Stahl, K., Collins, K., Hannaford, J., Acreman, M., Svoboda, M., Knutson, C., Smith, K.H., Wall, N., Fuchs, B., Crossman, N.D., Overton, I.C., 2016a. Drought indicators revisited: the need for a wider consideration of environment and society. WIREs Water 3, 516–536. https://doi.org/10.1002/wat2.1154.

Bachmair, S., Svensson, C., Hannaford, J., Barker, L.J., Stahl, K., 2016b. A quantitative analysis to objectively appraise drought indicators and model drought impacts. Hydrol. Earth Syst. Sci. 20, 2589–2609. https://doi.org/10.5194/hess-20-2589-2016.

Bachmair, S., Tanguy, M., Hannaford, J., Stahl, K., 2018. How well do meteorological indicators represent agricultural and forest drought across Europe? Environ. Res. Lett. 13 https://doi.org/10.1088/1748-9326/aaafda.

Beguería, S., Vicente-Serrano, S.M., Reig, F., Latorre, B., 2014. Standardized precipitation evapotranspiration index (SPEI) revisited: Parameter fitting, evapotranspiration models, tools, datasets and drought monitoring. Int. J. Climatol. 34 https://doi.org/10.1002/joc.3887.

Beguería, S., Tomas-Burguera, M., Serrano-Notivoli, R., Peña-Angulo, D., Vicente-Serrano, S.M., González-Hidalgo, J.-C., 2019. Gap filling of monthly temperature data and its effect on climatic variability and trends. J. Clim. 32, 7797–7821. https://doi.org/10.1175/JCLI-D-19-0244.1.

Berg, A., Sheffield, J., 2018. Climate change and drought: the soil moisture perspective. Curr. Clim. Chang. Reports 4, 180–191. https://doi.org/10.1007/s40641-018-0095-0.

Bhuyan-Erhardt, U., Erhardt, T.M., Laaha, G., Zang, C., Parajka, J., Menzel, A., 2019. Validation of drought indices using environmental indicators: streamflow and carbon flux data. Agric. For. Meteorol. 265, 218–226. https://doi.org/10.1016/j.agrformet.2018.11.016.

Bloomfield, J.P., Marchant, B.P., 2013. Analysis of groundwater drought building on the standardised precipitation index approach. Hydrol. Earth Syst. Sci. 17, 4769–4787. https://doi.org/10.5194/hess-17-4769-2013.

Bloomfield, J.P., Marchant, B.P., McKenzie, A.A., 2018. Increased incidence, duration and intensity of groundwater drought associated with anthropogenic warming. Hydrol. Earth Syst. Sci. Discuss. 2018, 1–23. https://doi.org/10.5194/hess-2018-244.

Bokal, S., Grobicki, A., Kindler, J., Thalmeinerova, D., 2014. From national to regional plans – the Integrated Drought Management Programme of the Global Water Partnership for Central and Eastern Europe. Weather Clim. Extrem. 3, 37–46. https://doi.org/10.1016/j.wace.2014.03.006.

Brandsma, T., 2014. Comparison of Automatic and Manual Precipitation Networks in the Netherlands.

Breshears, D.D., Adams, H.D., Eamus, D., Mcdowell, N.G., Law, D.J., Will, R.E., Williams, A.P., Zou, C.B., 2013. The critical amplifying role of increasing atmospheric moisture demand on tree mortality and associated regional die-off. Front. Plant Sci. 4 https://doi.org/10.3389/fpls.2013.00266.

Burke, E.J., 2011. Understanding the sensitivity of different drought metrics to the drivers of drought under increased atmospheric CO <inf>2</inf>. J. Hydrometeorol. 12, 1378–1394. https://doi.org/10.1175/2011JHM1386.1.

Cammalleri, C., Micale, F., Vogt, J., 2015. On the value of combining different modelled soil moisture products for European drought monitoring. J. Hydrol. 525, 547–558. https://doi.org/10.1016/j.jhydrol.2015.04.021.

Dai, A., Zhao, T., Chen, J., 2018. Climate change and drought: a precipitation and evaporation perspective. Curr. Clim. Chang. Reports 4, 301–312. https://doi.org/10.1007/s40641-018-0101-6.

De Luis, M., Vicente-Serrano, S., Gonzalez-Hidalgo, J., Raventós, J., 2003. Aplicación de las Tablas de Contingencia (Cross Tab análisis) al análisis espacial de tendencias climáticas. Cuad. Investig. Geográfica. 29, 23–34.

Dracup, J.A., 1991. Drought monitoring. Stoch. Hydrol. Hydraul. 5, 261–266. https://doi.org/10.1007/BF01543134.

Eamus, D., Boulain, N., Cleverly, J., Breshears, D.D., 2013. Global change-type drought-induced tree mortality: Vapor pressure deficit is more important than temperature per se in causing decline in tree health. Ecol. Evol. 3, 2711–2729. https://doi.org/10.1002/ece3.664.

Fang, B., Kansara, P., Dandridge, C., Lakshmi, V., 2021. Drought monitoring using high spatial resolution soil moisture data over Australia in 2015–2019. J. Hydrol. 594, 125960 https://doi.org/10.1016/j.jhydrol.2021.125960.

Ferguson, D.B., Masayesva, A., Meadow, A.M., Crimmins, M.A., 2016. Rain gauges to range conditions: collaborative development of a drought information system to support local decision-making. Weather Clim. Soc. 8, 345–359. https://doi.org/10.1175/WCAS-D-15-0060.1.

Folland, C.K., Hannaford, J., Bloomfield, J.P., Kendon, M., Svensson, C., Marchant, B.P., Prior, J., Wallace, E., 2015. Multi-annual droughts in the English Lowlands: a review of their characteristics and climate drivers in the winter half-year. Hydrol. Earth Syst. Sci. 19, 2353–2375. https://doi.org/10.5194/hess-19-2353-2015.

Ford, T.W., Quiring, S.M., 2019. Comparison of contemporary in situ, model, and satellite remote sensing soil moisture with a focus on drought monitoring. Water Resour. Res. 55, 1565–1582.

García-Herrera, R., Garrido-Pérez, J.M., Barriopedro, D., Ordóñez, C., Vicente-Serrano, S.M., Nieto, R., Gimeno, L., Sorí, R., Yiou, P., 2019. The European 2016/2017 drought. J. Clim. 32, 3169–3187.

Gouveia, C.M., Bastos, A., Trigo, R.M., Dacamara, C.C., 2012. Drought impacts on vegetation in the pre- and post-fire events over Iberian Peninsula. Nat. Hazards Earth Syst. Sci. 12, 3123–3137. https://doi.org/10.5194/nhess-12-3123-2012.

Gouveia, C.M., Páscoa, P., Russo, A., Trigo, R.M., 2016. Land degradation trend assessment over iberia during 1982-2012 | Evaluación de la tendencia a la degradación del suelo en Iberia durante 1982-2012. Cuad. Investig. Geogr. 42, 89–112. https://doi.org/10.18172/cig.2808.

Grossiord, C., Buckley, T.N., Cernusak, L.A., Novick, K.A., Poulter, B., Siegwolf, R.T.W., Sperry, J.S., McDowell, N.G., 2020. Plant responses to rising vapor pressure deficit. New Phytol. 226, 1550–1566. https://doi.org/10.1111/nph.16485.

Guttman, N.B., 1999. Accepting the standardized precipitation index: a calculation algorithm. JAWRA 35, 311–322. https://doi.org/10.1111/j.1752-1688.1999.tb03592.x.

Hannaford, J., Acreman, M., Stahl, K., Bachmair, S., Svoboda, M., Knutson, C., Crossman, N., Overton, I., Colloff, M., 2015. Enhancing Drought Monitoring and Early Warning by Linking Indicators to Impacts. https://doi.org/10.1201/b18077-49.

Hao, Z., AghaKouchak, A., Nakhjiri, N., Farahmand, A., 2014. Global integrated drought monitoring and prediction system. Sci. Data 1, 140001. https://doi.org/10.1038/sdata.2014.1.

Hao, Z., Hao, F., Singh, V.P., Ouyang, W., Cheng, H., 2017a. An integrated package for drought monitoring, prediction and analysis to aid drought modeling and assessment. Environ. Model. Softw. 91, 199–209. https://doi.org/10.1016/j.envsoft.2017.02.008.

Hao, Z., Yuan, X., Xia, Y., Hao, F., Singh, V.P., 2017b. An overview of drought monitoring and prediction systems at regional and global scales. Bull. Am. Meteorol. Soc. 98, 1879–1896. https://doi.org/10.1175/BAMS-D-15-00149.1.

Hayes, M.J., Svoboda, M.D., Wilhite, D.A., Vanyarkho, O.V., 1999. Monitoring the 1996 drought using the standardized precipitation index. Bull. Am. Meteorol. Soc. 80, 429–438. https://doi.org/10.1175/1520-0477(1999)080<0429:MTDUTS>2.0.CO;2.

Hayes, M., Svoboda, M., Wall, N., Widhalm, M., 2011. The Lincoln declaration on drought indices: Universal meteorological drought index recommended. Bull. Am. Meteorol. Soc. 92, 485–488. https://doi.org/10.1175/2010BAMS3103.1.

Heim, R.R., 2002. A review of twentieth-century drought indices used in the United States. Bull. Am. Meteorol. Soc. 83, 1149–1165. https://doi.org/10.1175/1520-0477(2002)083<1149:AROTDI>2.3.CO;2.

Heim, R., Brewer, M., 2012. The global drought monitor portal: the foundation for a global drought information system. Earth Interact. 16, 1–28. https://doi.org/10.1175/2012EI000446.1.

Hervás-Gámez, C., Delgado-Ramos, F., 2019. Drought management planning policy: from Europe to Spain. Sustainability 11, 1862. https://doi.org/10.3390/su11071862.

Ji, L., Peters, A.J., 2003. Assessing vegetation response to drought in the northern Great Plains using vegetation and drought indices. Remote Sens. Environ. 87, 85–98. https://doi.org/10.1016/S0034-4257(03)00174-3.

Lakshmi, V., Fayne, J., Bolten, J., 2018. A comparative study of available water in the major river basins of the world. J. Hydrol. 567, 510–532. https://doi.org/10.1016/j.jhydrol.2018.10.038.

Legates, D.R., DeLiberty, T.L., 1993. Precipitation measurement biases in the United States1. JAWRA 29, 855–861. https://doi.org/10.1111/j.1752-1688.1993.tb03245.x.

Leuzinger, S., Körner, C., 2010. Rainfall distribution is the main driver of runoff under future CO2-concentration in a temperate deciduous forest. Glob. Chang. Biol. 16, 246–254. https://doi.org/10.1111/j.1365-2486.2009.01937.x.

López-Moreno, J.I., Vicente-Serrano, S.M., Zabalza, J., Beguería, S., Lorenzo-Lacruz, J., Azorin-Molina, C., Morán-Tejeda, E., 2013. Hydrological response to climate variability at different time scales: a study in the Ebro basin. J. Hydrol. 477, 175–188. https://doi.org/10.1016/j.jhydrol.2012.11.028.

Lorenz, D.J., Otkin, J.A., Svoboda, M., Hain, C.R., Anderson, M.C., Zhong, Y., 2017. Predicting U.S. drought monitor states using precipitation, soil moisture, and evapotranspiration anomalies. Part I: development of a nondiscrete USDM index. J. Hydrometeorol. 18, 1943–1962. https://doi.org/10.1175/JHM-D-16-0066.1.

Lorenzo-Lacruz, J., Vicente-Serrano, S.M., López-Moreno, J.I., Beguería, S., García-Ruiz, J.M., Cuadrat-Prats, J.M., 2010. The impact of droughts and water management on various hydrological systems in the headwaters of the Tagus River (Central Spain). J. Hydrol. 386, 13–26. https://doi.org/10.1016/j.jhydrol.2010.01.001.

Lorenzo-Lacruz, J., Vicente-Serrano, S.M., González-Hidalgo, J.C., López-Moreno, J.I., Cortesi, N., 2013. Hydrological drought response to meteorological drought in the Iberian Peninsula. Clim. Res. 58 https://doi.org/10.3354/cr01177.

Lorenzo-Lacruz, J., Garcia, C., Morán-Tejeda, E., 2017. Groundwater level responses to precipitation variability in Mediterranean insular aquifers. J. Hydrol. 552, 516–531. https://doi.org/10.1016/J.JHYDROL.2017.07.011.

Manning, C., Widmann, M., Bevacqua, E., Van Loon, A.F., Maraun, D., Vrac, M., 2018. Soil moisture drought in Europe: a compound event of precipitation and potential evapotranspiration on multiple time scales. J. Hydrometeorol. 19, 1255–1271. https://doi.org/10.1175/JHM-D-18-0017.1.

McDowell, N.G., Allen, C.D., 2015. Darcy's law predicts widespread forest mortality under climate warming. Nat. Clim. Chang. 5, 669–672. https://doi.org/10.1038/nclimate2641.

McRoberts, D.B., Nielsen-Gammon, J.W., 2012. The use of a high-resolution standardized precipitation index for drought monitoring and assessment. J. Appl. Meteorol. Climatol. 51, 68–83. https://doi.org/10.1175/JAMC-D-10-05015.1.

Mishra, A.K., Singh, V.P., 2010. A review of drought concepts. J. Hydrol. 391, 202–216. https://doi.org/10.1016/j.jhydrol.2010.07.012.

Mol, A., Tait, A., Macara, G., 2017. An automated drought monitoring system for New Zealand. Weather Clim. 37, 23–36. https://doi.org/10.2307/26735444.

Mukherjee, S., Mishra, A., Trenberth, K.E., 2018. Climate change and drought: a perspective on drought indices. Curr. Clim. Chang. Reports 4, 145–163. https://doi.org/10.1007/s40641-018-0098-x.

Nijssen, B., Shukla, S., Lin, C., Gao, H., Zhou, T., Ishottama, Sheffield, J., Wood, E.F., Lettenmaier, D.P., 2014. A prototype global drought information system based on multiple land surface models. J. Hydrometeorol. 15, 1661–1676. https://doi.org/10.1175/JHM-D-13-090.1.

Noel, M., Bathke, D., Fuchs, B., Gutzmer, D., Haigh, T., Hayes, M., Poděbradská, M., Shield, C., Smith, K., Svoboda, M., 2020. Linking drought impacts to drought severity at the state level. Bull. Am. Meteorol. Soc. 101, E1312–E1321. https://doi.org/10.1175/BAMS-D-19-0067.1.

Noguera, I., Domínguez-Castro, F., Vicente-Serrano, S.M., 2021. Flash drought response to precipitation and atmospheric evaporative demand in Spain. Atmosphere (Basel). 12 https://doi.org/10.3390/atmos12020165.

Páscoa, P., Gouveia, C.M., Russo, A., Trigo, R.M., 2017. The role of drought on wheat yield interannual variability in the Iberian Peninsula from 1929 to 2012. Int. J. Biometeorol. 61, 439–451. https://doi.org/10.1007/s00484-016-1224-x.

Peña-Gallardo, M., Vicente-Serrano, S.M., Camarero, J.J., Gazol, A., Sánchez-Salguero, R., Domínguez-Castro, F., El Kenawy, A., Beguería-Portugés, S., Gutiérrez, E., de Luis, M., Sangüesa-Barreda, G., Novak, K., Rozas, V., Tíscar, P.A., Linares, J.C., del Castillo, E., Ribas Matamoros, M., García-González, I., Silla, F., Camisón, Á., Génova, M., Olano, J.M., Longares, L.A., Hevia, A., Galván, J.D., 2018. Drought sensitiveness on forest growth in Peninsular Spain and the Balearic Islands. Forests 9.

Peña-Gallardo, M., Vicente-Serrano, S.M., Dominguez-Castro, F., Begueria, S., Martín Vicente-Serrano, S., Domínguez-Castro, F., Beguería, S., 2019. The impact of drought

on the productivity of two rainfed crops in Spain. Nat. Hazards Earth Syst. Sci. 19, 1215–1234. https://doi.org/10.5194/nhess-19-1215-2019.
Pereira, L.S., Allen, R.G., Smith, M., Raes, D., 2015. Crop evapotranspiration estimation with FAO56: past and future. Agric. Water Manag. 147, 4–20. https://doi.org/10.1016/j.agwat.2014.07.031.
Phillips, D.L., Dolph, J., Marks, D., 1992. A comparison of geostatistical procedures for spatial analysis of precipitation in mountainous terrain. Agric. For. Meteorol. 58, 119–141. https://doi.org/10.1016/0168-1923(92)90114-J.
Potopová, V., Boroneanţ, C., Boincean, B., Soukup, J., 2016. Impact of agricultural drought on main crop yields in the Republic of Moldova. Int. J. Climatol. 36, 2063–2082. https://doi.org/10.1002/joc.4481.
Pozzi, W., Sheffield, J., Stefanski, R., Cripe, D., Pulwarty, R., Vogt, J.V., Heim, R.R., Brewer, M.J., Svoboda, M., Westerhoff, R., van Dijk, A.I.J.M., Lloyd-Hughes, B., Pappenberger, F., Werner, M., Dutra, E., Wetterhall, F., Wagner, W., Schubert, S., Mo, K., Nicholson, M., Bettio, L., Nunez, L., van Beek, R., Bierkens, M., de Goncalves, L.G.G., de Mattos, J.G.Z., Lawford, R., 2013. Toward global drought early warning capability: expanding international cooperation for the development of a framework for monitoring and forecasting. Bull. Am. Meteorol. Soc. 94, 776–785. https://doi.org/10.1175/BAMS-D-11-00176.1.
Pulwarty, S.R., Sivakumar, M.V.K., 2014. Information systems in a changing climate: early warnings and drought risk management. Weather Clim. Extrem. 3, 14–21. https://doi.org/10.1016/j.wace.2014.03.005.
Quiring, S.M., Papakryiakou, T.N., 2003. An evaluation of agricultural drought indices for the Canadian prairies. Agric. For. Meteorol. 118, 49–62. https://doi.org/10.1016/S0168-1923(03)00072-8.
Ribeiro, A.F.S., Russo, A., Gouveia, C.M., Páscoa, P., 2019. Modelling drought-related yield losses in Iberia using remote sensing and multiscalar indices. Theor. Appl. Climatol. 136, 203–220. https://doi.org/10.1007/s00704-018-2478-5.
Scaini, A., Sánchez, N., Vicente-Serrano, S.M., Martínez-Fernández, J., 2015. SMOS-derived soil moisture anomalies and drought indices: a comparative analysis using in situ measurements. Hydrol. Process. 29 https://doi.org/10.1002/hyp.10150.
Seneviratne, S.I., Ciais, P., 2017. Trends in ecosystem recovery from drought. Nature 548, 164.
Sevruk, B., Ondrás, M., Chvíla, B., 2009. The WMO precipitation measurement intercomparisons. Atmos. Res. 92, 376–380. https://doi.org/10.1016/j.atmosres.2009.01.016.
Shah, R.D., Mishra, V., 2022. Development of an experimental near-real-time drought monitor for India. J. Hydrometeorol. 16, 327–345. https://doi.org/10.1175/JHM-D-14-0041.1 n.d.
Sheffield, J., Wood, E.F., Chaney, N., Guan, K., Sadri, S., Yuan, X., Olang, L., Amani, A., Ali, A., Demuth, S., Ogallo, L., 2014. A drought monitoring and forecasting system for Sub-Sahara African water resources and food security. Bull. Am. Meteorol. Soc. 95, 861–882. https://doi.org/10.1175/BAMS-D-12-00124.1.
Stagge, J.H., Tallaksen, L.M., Gudmundsson, L., Van Loon, A.F., Stahl, K., 2015. Candidate distributions for climatological drought indices (SPI and SPEI). Int. J. Climatol. 35, 4027–4040. https://doi.org/10.1002/joc.4267.
Svoboda, M., Hayes, M., Wilhite, D., 2001. The role of integrated drought monitoring in drought mitigation planning. Ann. Arid Zone 40, 1–11.
Svoboda, M., LeComte, D., Hayes, M., Heim, R., Gleason, K., Angel, J., Rippey, B., Tinker, R., Palecki, M., Stooksbury, D., Miskus, D., Stephens, S., 2002. The drought monitor. Bull. Am. Meteorol. Soc. 83, 1181–1190. https://doi.org/10.1175/1520-0477(2002)083<1181:TDM>2.3.CO;2.
Talchabhadel, R., Karki, R., Parajuli, B., 2016. Intercomparison of precipitation measured between automatic and manual precipitation gauge in Nepal. Measurement 106. https://doi.org/10.1016/j.measurement.2016.06.047.
Tallaksen, L.M., Stahl, K., 2014. Spatial and temporal patterns of large-scale droughts in Europe: Model dispersion and performance. Geophys. Res. Lett. 41, 429–434. https://doi.org/10.1002/2013GL058573.
Tallaksen, L.M., Madsen, H., Clausen, B., 1997. On the definition and modelling of streamflow drought duration and deficit volume. Hydrol. Sci. J. 42, 15–33. https://doi.org/10.1080/02626669709492003.
Tian, L., Yuan, S., Quiring, S.M., 2018. Evaluation of six indices for monitoring agricultural drought in the south-Central United States. Agric. For. Meteorol. 249, 107–119. https://doi.org/10.1016/J.AGRFORMET.2017.11.024.
Tomas Burguera, M., Jiménez Castañeda, A., Luna Rico, Y., Morata Gasca, A., Vicente-Serrano, S.M., González Hidalgo, J.C., Begueria, S., 2016. Control de calidad de siete variables del banco nacional de datos de AEMET. In: Jorge, Olcina Cantos, Rico Amorós Antonio, M., Moltó Mantero, E. (Eds.), Clima, Sociedad, Riesgos y Ordenación Del Territorio. Instituto Interuniversitario de Geografía. Universidad de Alicante; [Sevilla]: Asociación Española de Climatología, Alicante, pp. 407–415.
Tomas-Burguera, M., Vicente Serrano, S.M., Peña-Angulo, D., Domínguez-Castro, F., Noguera, I., El Kenawy, A., 2020. Global characterization of the varying responses of the Standardized Evapotranspiration Index (SPEI) to atmospheric evaporative demand (AED). J. Geophys. Res. Atmos. https://doi.org/10.1029/2020JD033017 n/a, e2020JD033017.
Turco, M., Jerez, S., Donat, M.G., Toreti, A., Vicente-Serrano, S.M., Doblas-Reyes, F.J., 2020. A global probabilistic dataset for monitoring meteorological droughts. Bull. Am. Meteorol. Soc. 101, E1628–E1644. https://doi.org/10.1175/BAMS-D-19-0192.1.
Valík, A., Brázdil, R., Zahradníček, P., Tolasz, R., Fiala, R., 2021. Precipitation measurements by manual and automatic rain gauges and their influence on homogeneity of long-term precipitation series. Int. J. Climatol. 41, E2537–E2552. https://doi.org/10.1002/joc.6862.
Van Loon, A.F., 2015. Hydrological drought explained. Wiley Interdiscip. Rev. Water 2, 359–392. https://doi.org/10.1002/wat2.1085.
Vicente-Serrano, S.M., 2021. The complex multi-sectoral impacts of drought: Evidence from a mountainous basin in the Central Spanish Pyrenees. Sci. Total Environ. 769, 144702.
Vicente-Serrano, S.M., Beguería, S., 2016. Comment on "Candidate distributions for climatological drought indices (SPI and SPEI)" by James H. Stagge et al. Int. J. Climatol. 36 https://doi.org/10.1002/joc.4474.
Vicente-Serrano, S.M., López-Moreno, J.I., 2005. Hydrological response to different time scales of climatological drought: an evaluation of the standardized Precipitation Index in a mountainous Mediterranean basin. Hydrol. Earth Syst. Sci. 9 https://doi.org/10.5194/hess-9-523-2005.
Vicente-Serrano, S.M., Beguería, S., López-Moreno, J.I., 2010. A multiscalar drought index sensitive to global warming: the standardized precipitation evapotranspiration index. J. Clim. 23 https://doi.org/10.1175/2009JCLI2909.1.
Vicente-Serrano, S.M., Beguería, S., Lorenzo-Lacruz, J., Camarero, J.J., López-Moreno, J. I., Azorin-Molina, C., Revuelto, J., Morán-Tejeda, E., Sanchez-Lorenzo, A., 2012. Performance of drought indices for ecological, agricultural, and hydrological applications. Earth Interact. 16 https://doi.org/10.1175/2012EI000434.1.
Vicente-Serrano, S.M., Azorin-Molina, C., Sanchez-Lorenzo, A., Revuelto, J., Morán-Tejeda, E., López-Moreno, J.I., Espejo, F., 2014a. Sensitivity of reference evapotranspiration to changes in meteorological parameters in Spain (1961-2011). Water Resour. Res. 50 https://doi.org/10.1002/2014WR015427.
Vicente-Serrano, Sergio M., Lopez-Moreno, J.-I., Beguería, S., Lorenzo-Lacruz, J., Sanchez-Lorenzo, A., García-Ruiz, J.M., Azorin-Molina, C., Morán-Tejeda, E., Revuelto, J., Trigo, R., Coelho, F., Espejo, F., 2014b. Evidence of increasing drought severity caused by temperature rise in southern Europe. Environ. Res. Lett. 9, 044001 https://doi.org/10.1088/1748-9326/9/4/044001.
Vicente-Serrano, Sergio M., Tomas-Burguera, M., Beguería, S., Reig, F., Latorre, B., Peña-Gallardo, M., Luna, M.Y., Morata, A., González-Hidalgo, J.C., 2017a. A high resolution dataset of drought indices for Spain. Data 2.
Vicente-Serrano, S.M., Zabalza-Martínez, J., Borràs, G., López-Moreno, J.I., Pla, E., Pascual, D., Savé, R., Biel, C., Funes, I., Azorin-Molina, C., Sanchez-Lorenzo, A., Martín-Hernández, N., Peña-Gallardo, M., Alonso-González, E., Tomas-Burguera, M., El Kenawy, A., 2017b. Extreme hydrological events and the influence of reservoirs in a highly regulated river basin of northeastern Spain. J. Hydrol. Reg. Stud. 12, 13–32. https://doi.org/10.1016/j.ejrh.2017.01.004.
Vicente-Serrano, S.M.M., Azorin-Molina, C., Peña-Gallardo, M., Tomas-Burguera, M., Dominguez-Castro, F., Martin-Hernández, N., Begueria, S., El Kenawy, A., Noguera, I., Garcia, M., Domínguez-Castro, F., Martín-Hernández, N., Beguería, S., El Kenawy, A., Noguera, I., García, M., 2019. A high-resolution spatial assessment of the impacts of drought variability on vegetation activity in Spain from 1981 to 2015. Nat. Hazards Earth Syst. Sci. 19, 1189–1213. https://doi.org/10.5194/nhess-19-1189-2019.
Vicente-Serrano, S.M., McVicar, T.R., Miralles, D.G., Yang, Y., Tomas-Burguera, M., 2020a. Unraveling the influence of atmospheric evaporative demand on drought and its response to climate change. Wiley Interdiscip. Rev. Clim. Chang. 11 https://doi.org/10.1002/wcc.632.
Vicente-Serrano, Sergio M., McVicar, T.R., Miralles, D.G., Yang, Y., Tomas-Burguera, M., 2020b. Unraveling the influence of atmospheric evaporative demand on drought and its response to climate change. WIREs Clim. Chang. 11, e632 https://doi.org/10.1002/wcc.632.
Wang, K., Dickinson, R.E., Liang, S., 2012. Global atmospheric evaporative demand over land from 1973 to 2008. J. Clim. 25, 8353–8361. https://doi.org/10.1175/JCLI-D-11-00492.1.
Wang, H., Vicente-serrano, S.M., Tao, F., Zhang, X., Wang, P., Zhang, C., Chen, Y., Zhu, D., Kenawy, A.E., 2016. Monitoring winter wheat drought threat in Northern China using multiple climate-based drought indices and soil moisture during 2000–2013. Agric. For. Meteorol. 228–229. https://doi.org/10.1016/j.agrformet.2016.06.004.
Wang, Y., Lv, J., Hannaford, J., Wang, Y., Sun, H., Barker, L.J., Ma, M., Su, Z., Eastman, M., 2020. Linking drought indices to impacts to support drought risk assessment in Liaoning province, China. Nat. Hazards Earth Syst. Sci. 20, 889–906. https://doi.org/10.5194/nhess-20-889-2020.
Wilhite, D.A., 2002. Combating drought through preparedness. Nat. Resour. Forum 26, 275–285. https://doi.org/10.1111/1477-8947.00030.
Wilhite, D., 2007. Preparedness and coping strategies for agricultural drought risk management: recent progress and trends. Manag. Weather Clim. Risks Agric. 21–38. https://doi.org/10.1007/978-3-540-72746-0_2.
Wilhite, D.A., 2009. Drought monitoring as a component of drought preparedness planning. In: Iglesias, A., Cancelliere, A., Wilhite, D.A., Garrote, L., Cubillo, F. (Eds.), Coping with Drought Risk in Agriculture and Water Supply Systems: Drought Management and Policy Development in the Mediterranean. Springer, Netherlands, Dordrecht, pp. 3–19. https://doi.org/10.1007/978-1-4020-9045-5_1.
Wilhite, D.A., Svoboda, M.D., Hayes, M.J., 2007. Understanding the complex impacts of drought: a key to enhancing drought mitigation and preparedness. Water Resour. Manag. 21, 763–774. https://doi.org/10.1007/s11269-006-9076-5.
Williams, A.P., Allen, C.D., Macalady, A.K., Griffin, D., Woodhouse, C.A., Meko, D.M., Swetnam, T.W., Rauscher, S.A., Seager, R., Grissino-Mayer, H.D., Dean, J.S., Cook, E. R., Gangodagamage, C., Cai, M., Mcdowell, N.G., 2013. Temperature as a potent driver of regional forest drought stress and tree mortality. Nat. Clim. Chang. 3, 292–297. https://doi.org/10.1038/nclimate1693.
Willmott, C.J., Robeson, S.M., Matsuura, K., 2012. A refined index of model performance. Int. J. Climatol. 32 (13), 2088–2094.
WMO, 2012. Standardized Precipitation Index User Guide (M. Svoboda, M. Hayes and D. Wood). Geneva.
Wood, E.F., Schubert, S.D., Wood, A.W., Peters-Lidard, C.D., Mo, K.C., Mariotti, A., Pulwarty, R.S., 2015. Prospects for advancing drought understanding, monitoring,

and prediction. J. Hydrometeorol. 16, 1636–1657. https://doi.org/10.1175/JHM-D-14-0164.1.

Yan, N., Wu, B., Boken, V.K., Chang, S., Yang, L., 2016. A drought monitoring operational system for China using satellite data: design and evaluation. Geomatics Nat. Hazards Risk 7, 264–277. https://doi.org/10.1080/19475705.2014.895964.

Yuan, S., Quiring, S.M., 2017. Evaluation of soil moisture in CMIP5 simulations over the contiguous United States using in situ and satellite observations. Hydrol. Earth Syst. Sci. 21, 2203–2218. https://doi.org/10.5194/hess-21-2203-2017.

Yuan, S., Quiring, S.M., Zhao, C., 2020. Evaluating the utility of drought indices as soil moisture proxies for drought monitoring and land–atmosphere interactions. J. Hydrometeorol. 21, 2157–2175. https://doi.org/10.1175/JHM-D-20-0022.1.

Zhang, Q., Kong, D., Singh, V.P., Shi, P., 2017a. Response of vegetation to different time-scales drought across China: Spatiotemporal patterns, causes and implications. Glob. Planet. Chang. 152, 1–11. https://doi.org/10.1016/j.gloplacha.2017.02.008.

Zhang, L., Zhang, H., Zhang, Q., Li, Y., Zhao, J., 2017b. On the potential application of land surface models for drought monitoring in China. Theor. Appl. Climatol. 128, 649–665. https://doi.org/10.1007/s00704-016-1730-0.

Zink, M., Samaniego, L., Kumar, R., Thober, S., Mai, J., Schäfer, D., Marx, A., 2016. The German drought monitor. Environ. Res. Lett. 11, 074002 https://doi.org/10.1088/1748-9326/11/7/074002.